Journal of Materials Chemistry B

Accepted Manuscript

ROYAL SOCIETY OF CHEMISTRY

www.rsc.org/materialsB

Tunable, Bioactive Protein Conjugated Hyaluronic Acid Hydrogels for Neural Engineering Applications

Dalia Shendi[1], Ana Dede[1], Yuan Yin[1], Chaoming Wang[1], Chandra Valmikinathan[2], Anjana Jain[1*]

1. nano-Neural Therapeutics Laboratory, Department Biomedical Engineering, Worcester Polytechnic Institute, Worcester, MA
2. ACell Inc., Columbia, MD

Running Title: Tunable, Bioactive HA Hydrogels

A total of 32 Pages and 12 Figures

* Correspondence should be addressed to:

Anjana Jain, Ph.D.
Assistant Professor of Biomedical Engineering
nano-Neural Therapeutics Laboratory
Department of Biomedical Engineering
Worcester Polytechnic Institute
100 Institute Road
Worcester, MA 01609
Ph: 508-831-4956
Fax: 508-831-4121
Email: ajain@wpi.edu

Abstract

Millions of Americans suffer from nervous system injuries. Hydrogels have been investigated to (1) bridge nerve gaps; (2) act as a scaffold for bioactive molecule delivery or cell transplantation; and/or (3) promote axonal outgrowth. In this study, we use a rapid, one-step Michael addition click chemistry reaction to fabricate a hyaluronic acid (HA) scaffold for neural repair. Briefly, some of the primary hydroxyl groups on the HA backbone were modified to a vinyl sulfone functional group for (1) conjugation of thiol based bioactive molecules and (2) hydrogel crosslinking, which was confirmed by Proton Nuclear Magnetic Resonance (1H-NMR) and Fourier Transform Infrared Spectroscopy (FTIR). The degree of crosslinking creates a mechanically tunable hydrogel. Rheology confirmed that the storage modulus was within the order of magnitude to that of nervous tissue. Primary human dermal fibroblasts and primary mouse neural stem cells (NSCs) seeded in the HA hydrogel were viable and proliferative, thus demonstrating that the HA hydrogel is conducive as a scaffold for cell transplantation. The range in pore size demonstrated that the scaffold supports cell migration and neurite extension. Neurite outgrowth of cultured whole embryonic day 9 chick dorsal root ganglions signifies that the hydrogel supports axonal outgrowth. Reduction in immune and inflammatory cell viability was observed in anti-Fas-conjugated HA hydrogel, whereas the NSCs maintained viability in the anti-Fas HA hydrogel. Therefore, this one-step, rapid, controllable reaction is an efficient method for fabrication of tunable, biomolecule conjugated hydrogels for neural engineering applications.

1. Introduction

Approximately 2.5 million people suffer from central nervous system (CNS) injuries, such as traumatic brain injury, spinal cord injury, and stroke, as well as peripheral nerve injuries annually in the United States[1-3]. Biodegradable hydrogels have been investigated as potential scaffolds due to similar mechanical properties with nervous tissue in order to bridge the created gap or void space. Additionally, hydrogels can serve as delivery vehicles for cells and/or protein due to their water solubility and porous architecture after gelation *in vivo*. One of the main characteristics when selecting a hydrogel for nervous system applications is that it polymerizes in situ, thereby, conforming to the shape of the defect, minimizing the interfaces for re-growing axons and migrating cells[4]. There are several material candidates used as hydrogel scaffolds for neural applications, such as agarose[4-7], methylcellulose[8], collagen[9], hyaluronic acid (HA)[10-12] and polyethylene glycol[13]. These hydrogels have several advantages and disadvantages as scaffolds for neural repair. HA has been used in this study as the backbone for the hydrogel scaffold as it is abundantly found in the extracellular matrix (ECM), especially in nervous system tissue[14]. HA as a hydrogel has several advantages: (1) net negative charge[15, 16], (2) anti-inflammatory properties[17]; and (3) hydrophilicity[18]. The net negative charge is important for swelling and permeability[19]. The anti-inflammatory properties aid in reduction of T-cell and macrophage recruitment, thus making it beneficial for nervous tissue repair and cell transplantation. The hydrophilicity of the HA hydrogel minimizes protein and host cell deposition[18]. HA hydrogels have previously been utilized in neural engineering and have demonstrated to be beneficial for cell transplantation and differentiation of neural progenitor cells, as well as a scaffold for spinal cord injury[11, 20].

Various methods to crosslink HA for gelation, such as photocrosslinking[21, 22] and chemical crosslinking of modified HA backbone[23-26] have been used. These crosslinking methods require functional group modifications to the HA backbone, such as with acrylates and thiols. Acrylate group modifications to the hydrogel are common to allow for protein modifications. However, previous methodology reported for acrylation is lengthy, on the order of hours to days[11] and some of the protocols involve a two-step process[27], which require removing unreacted chemicals prior to the second step. Functionalizing the backbone of the HA polymer with vinyl sulfone (VS) groups is an ideal method for hydrogel fabrication because it is quick, and lends to further modification with proteins and antibodies[28].

In this study, we used a quick one-step method for fabrication of a VS-modified hydrogel scaffold suitable for bioactive molecule conjugation. Vinyl sulfone groups were added to the HA backbone in a controlled 20 minute one-step reaction. With the addition of the VS groups to the HA backbone, bioactive molecules can then be conjugated to the HA solution without affecting its crosslinking potential. The antibody to Fas, an apoptotic promoting protein, was conjugated to the VS modified HA (HA-VS) backbone using 42% of the total available VS groups to produce an immuno-modulating and neuroprotective hydrogel scaffold. The HA precursor solution was polymerized by reacting the remaining vinyl sulfone groups on the HA with 4-arm PEG-thiol (PEG-thiol). The crosslinker minimized gelation time after biomolecule conjugation[29]. Through modification of the crosslinker percentage, properties such as gelation kinetics, mechanical integrity, and hydrogel microstructure can be controlled to produce a suitable hydrogel scaffold. This reaction mechanism for fabrication of hydrogels is also applicable for other polymers with primary hydroxyl groups in the backbone that are used for

neural engineering applications for *in vivo* applications, such as cell transplantation and drug delivery.

2. Experimental

2.1 Materials

Hyaluronic acid, divinyl sulfone (DVS), and PEG-thiol were purchased from Lifecore Biomedical, Sigma Aldrich, and JenKem, respectively. Dialysis membranes were purchased from Spectrum Labs. Hyaluronidase used for the degradation studies was purchased from Worthington Biochem. Mouse neural stem cells (NSCs) were purchased from Cyagen. Primary human dermal fibroblasts (CT-1005) were a generous donation from Tanja Dominko (Worcester Polytechnic Institute). Microglial cells (C8B4) and Jurkat cells were purchased from ATCC. Live/Dead assay kit was purchased from Life Technologies. Primary and secondary antibodies used were purchased from AbCam and LifeTech, respectively.

2.2 Fabrication of Hyaluronic Acid Hydrogel Precursor Solutions

To fabricate HA-VS hydrogel precursor solution, HA (1×10^6 Da) was first dissolved in 0.01 N sodium hydroxide (NaOH) for a working concentration of 1% (w/v). The HA solution reacted with the DVS for 20 min at room temperature. The reaction was quenched with 1 N HCl until the pH level reached 5. The solution was dialyzed (MWCO 25kD) for 48 hrs at 4°C to remove excess DVS. The HA-VS solution was then lyophilized and stored at -20^{o} C until ready to use.

In order to fabricate anti-Fas HA hydrogel precursor, 250 ng/mL of anti-Fas was added to reconstituted 0.75% (w/v) HA solution. The conjugation reaction occurred under rotation at

37°C for 1 hr. Samples were dialyzed for 24 hrs, lyophilized, and stored in -20 ^{o}C until use. The precursor solution was crosslinked with 1% PEG-thiol (1 x 10^4 Da) at a 1:1 ratio to create a hydrogel unless otherwise specified.

2.3 FTIR Analysis for Addition of Vinyl Sulfone Groups

To confirm the addition of vinyl sulfone groups to HA, FTIR was performed on the samples. A 1% (w/v) solution of pure (uncrosslinked) HA and HA-VS were prepared as mentioned in the section above. The HA and HA-VS were analyzed using Thermo Scientific ATR-FTIR. A resolution of 4 cm-1 was used, and read between 400 and 4000 cm-1. A total of 16 iterations for each sample were averaged to obtain FTIR spectrum. Prior to reading the samples, the FTIR was calibrated and air was read as background. Peak identifier software was used to identify the peaks.

2.4 1H NMR Analysis for Degree of Vinyl Sulfone Modification and Anti-Fas Conjugation

1H-NMR (Bruker BioSpin) was performed to determine the degree of vinyl sulfone modification to the HA backbone, and conjugation of anti-Fas. Degree of vinyl sulfone modification was analyzed by varying the molar excess of DVS, as well as the reaction time of HA with DVS. The following molar excesses of DVS were used and reacted for 20 min: 1M, 2M, 3M, 6M, and 10M. The following reaction times were used to determine the effect on degree of vinyl sulfone modification for 3 M excess DVS: 10 min, 15, min, 20 min, 25 min, 30 min and 40 min. After lyophilization, the HA was reconstituted in deuterium oxide (D_2O) at a concentration of 7.5 mg/mL. The samples were analyzed for degree of VS modification using the Bruker BioSpin 500M Hz Avance III Digital NMR spectrometer. A total of 512 scans was

performed and then averaged together to obtain the H-NMR spectrum. Previously published methodology was used to calculate the degree of VS modification[11, 28, 30, 31]. Briefly, the ratio of the integrated area of the CH_2 peak of the vinyl sulfone groups at 6.0 to 6.5 ppm to the H3-H_6 peaks of solution HA-VS between 1.65 and 2 ppm was calculated.

1H-NMR was also performed to determine the conjugation of anti-Fas to the HA backbone relative to the HA-VS sample. Soluble anti-Fas was analyzed at 250ng/mL to determine the NMR molecular signal prior to conjugation. Anti-Fas (250 ng/mL) was conjugated to 0.75% (w/v) HA. The anti-Fas was allowed to bind to the HA-VS solution for 20 min, 40 min, 60 min, or 120 min. Samples were then lyophilized and reconstituted in D_2O for NMR analysis. Anti-Fas binds to the VS groups on the HA-VS backbone, thus the vinyl sulfone peaks were used to quantify the degree of conjugation. A reduction in the ratio of peaks indicates binding of the bioactive molecule. The degree of anti-Fas conjugation was calculated similarly to the degree of modification study specified above, and normalized relative to the HA-VS control group. Anti-Fas conjugated hydrogel was crosslinked with 1% (w/v) PEG-thiol to form the hydrogel, and confirm the availability of VS groups for crosslinking chemistry.

2.5 Determination of Hydrogel Morphology by Optical and Scanning Electron Microscopy

The HA hydrogels were prepared as previously described in section 2.2. Digital images of the hydrogel were taken to show the gel properties and the optical transparency of the hydrogels. Optical transparency is a desired property for neural engineering applications, as it allows for easy imaging of transplanted cells within the hydrogels. For SEM, 0.75% (w/v) HA and various percentages of PEG-thiol (1%, 5%, and 20% w/v) were mixed in a 1:1 volume ratio, flash frozen in liquid nitrogen, and then immediately lyophilized. All the samples were mounted

onto aluminum stubs and sputter-coated with gold-palladium for 60s at 25mA prior to observation. SEM (JSM-7000F, operated at an accelerating voltage of 3kV) was used to study the morphology of the hydrogels. Several magnifications were obtained to study the surface properties and the pore dimensions and sizes.

2.6 Characterization of Swelling and Degradation of HA Hydrogel

Ten millimeter HA hydrogel discs were prepared for the swelling studies. The samples of 0.75% HA with 20% PEG thiol, 15% PEG thiol, 5 % PEG thiol, and 1% PEG thiol were prepared. To determine the optimal HA percentage, hydrogels with 0.5% HA, 0.75% HA, and 1% HA were crosslinked with 1% PEG thiol. The following volumetric ratios of 0.75% HA and 1% PEG-thiol were analyzed: 1:1, 3:1, and 7:1. The dry weight (W_d) was measured prior to swelling in distilled deionized water (DI H_2O) at 37 °C. The mass of the HA hydrogel discs (W_s, swollen weight) was measured at 3 hrs, 6 hrs, 12 hrs, 24 hrs, 48 hrs, 72 hrs, and 96 hrs. The swelling percentage of the hydrogel was calculated using the following equation:

$$\% \text{ Swelling} = (W_s/W_d) * 100$$

For the degradation studies, similar conditions were used as specified in the swelling studies. Hydrogels were swelled in PBS without the enzyme. The initial weight of the hydrogels was recorded (W_d) prior to swelling for 24 hours in PBS at 37°C. After 24 hrs, hyaluronidase (10U/mL) was added to each well as previously described[32]. Samples were weighed (W_s) every 24 hrs for 3 consecutive days. An n=3 per condition was used to determine the degradation percent of the hydrogels. The percentage of degradation of the hydrogel was calculated using the following equation:

$$\%\text{Degradation} = (W_s/Wd) \times 100$$

2.7 Analysis of Mechanical Properties using Rheology

For the rheological studies, the Discovery Hybrid Rheometer HR-3A with a parallel plate (12 mm plate) configuration was used to analyze the storage modulus of the hydrogels. Four hundred microliters of HA hydrogel was loaded on to the stage. An amplitude sweep of 1 Hz and an oscillation strain from 1-1000% was performed. Samples with varied percentages (w/v) of PEG-thiol or HA were analyzed, as well as 1:1, 3:1 and 7:1 volume ratios of 0.75% HA crosslinked with 1% PEG-thiol.

2.8 Characterization of Cell Viability and Proliferation in HA Hydrogels

Mouse NSCs were passaged as neurospheres in NSC basal media supplemented with 1% (v/v) B27supplement, 10μg/mL epidermal growth factor (EGF) 5μg/mL fibroblast growth factor (FGF-β), 0.2% (w/v) heparin, and 1% (v/v) penicillin/streptomycin (PS/Strep). Neurospheres were dissociated using TrypeLE prior to encapsulation in HA hydrogel. The CT-1005 (passages 4-6) and C8B4 (passage 5-10) were cultured and maintained in DMEM supplemented with 10% (v/v) fetal bovine serum (FBS) and 1% (v/v) PS/Strep. Jurkat cells were maintained and cultured in RPMI 1640 media supplemented with 10% (v/v) FBS and 1% (v/v) PS/Strep.

The effect of the HA hydrogel on cell viability was determined by culturing the CT-1005 and mouse NSCs in a 4-well plate for 24 and 48 hrs. For both primary cell cultures, 150,000 cells were seeded in 200 μL of the reconstituted 0.75% HA hydrogel precursor solution crosslinked with 1% PEG-thiol at a 1:1 ratio. Cells were encapsulated within the partially crosslinked HA hydrogel and incubated at 37°C to allow completion of gelation. After the hydrogel fully crosslinked (5 mins), media was added to the wells. Twenty-four hours and 48

hrs post-seeding, the Live/Dead Assay was performed, and then fixed with 4% paraformaldehyde prior to storage at 4°C (n = 4).

Live/Dead assay was also performed on Jurkat cells, C8B4, and NSCs encapsulated in anti-Fas (250 ng/mL) conjugated HA hydrogel precursor solution. Similar procedure was performed as stated above; however, 250,000 cells were encapsulated in the HA only- and anti-Fas conjugated HA hydrogel precursor solution for 24 hours (n=3), and fixed with 4% paraformaldehyde.

Cell proliferation was assessed 24 and 48 hrs post-seeding in the HA hydrogel using an antibody against Ki-67, a marker for cell proliferation. Briefly, after fixing the samples with 4% paraformaldehyde, the hydrogel cultures were permeabilized and blocked with 10% goat serum in 0.1% Triton-X 100 for 1hr. The culture samples were incubated overnight at 4°C with primary antibody and then stained with goat anti-rabbit IgG AlexaFluor 488 for 2hrs. Hoechst was used as the nuclear stain (n=4). All images were acquired using the Zeiss Axiovert microscope with a Zeiss AxioCam MRm CCD camera.

2.9 Neurite Outgrowth of Dorsal Root Ganglia

To determine if the HA hydrogel support neurite outgrowth, embryonic day 9 (E9) Whitehorn chick DRGs were cultured within the hydrogel (0.75% HA and 1% PEG-thiol) for a 3 dimensional (3D) culture. The DRGs were explanted from the chick and mixed into 250 μL of HA hydrogel solution while the HA hydrogel was crosslinking with the PEG-thiol and seeded in 24-well plates for 48 hrs incubation. Neurobasal media containing 1% (v/v) B-27 supplement, 1% (v/v) L-glutamine, 1% (v/v) PS/Strep, and 40 ng/mL of nerve growth factor (NGF) was used. The images of the neurites were analyzed to obtain the 8 longest neurites on each DRG as

described by Yu *et al* [33]. There was n =3 wells per condition and each well contained 4 to 6 DRGs.

2.10 Statistical Analysis

Statistical analysis was performed to determine significance amongst the experimental conditions using GraphPad software. T-test was performed for the DRG neurite experiment. One-way analysis of variance (ANOVA) was conducted for hydrogel rheology, swelling, degradation, degree of VS modification, and degree of conjugation experiments. All data was considered significant for $p<0.05$. Post-hoc Tukey's test was performed for swelling and degradation, rheology, and NMR quantification experiments. Letters were used to denote the statistical significance of $p<0.05$ between different samples as indicated.

3. Results and Discussion

The objective of this study was to conjugate a bioactive molecule to a tunable, rapid in situ gelling HA hydrogel using a quick one-step reaction for neural engineering applications. This was implemented by adding vinyl sulfone groups to the HA backbone in a 20 min one-step Michael addition reaction. The HA-VS hydrogel is tunable due to the percentage of PEG-thiol crosslinker, which allows for changes in the mechanical properties of the hydrogel as well as gelation times. The ability to control the gelling parameters and kinetics is important as the application can be tailored for cell delivery in the neural system, as well as other regenerative medicine applications, such as cardiovascular, cartilage, and organ repairs.

3.1 Characterization of HA Hydrogel Acrylation and Protein Conjugation

The addition of VS the backbone of the HA at the hydroxyl position is seen in the reaction scheme in Figure 1A. Briefly, a Michael addition reaction was performed to allow the reaction between the DVS and the HA. Figure 1B shows the reaction schematic for conjugation of a thiol containing biomolecule. The inherent thiol groups in the bioactive molecule conjugate to the vinyl sulfone on the HA backbone. The HA molecule's signature and vinyl sulfone was confirmed using FTIR. The FTIR spectrum of HA only, DVS, and HA-VS solution can be seen in Figure 2. The spectrum obtained from the HA and DVS samples is the same as in literature[34, 35]. In the bottom spectrum for the HA-VS, the characteristic DVS peak is present at 1521. NMR was also performed to confirm the presence of the vinyl sulfone group, and quantify the degree of modification from the Michael addition. The addition of DVS to the HA backbone can be seen in the double peak located between 6 and 7 ppm. (Fig. 3A) The degree of VS modification of HA was calculated from the spectrum for the various hydrogels with DVS molar excesses and different reaction times (Fig. 3B-C). As seen in the molar excess experiments, a significant difference in degree of modification was observed for the 2M, 3M, 6M, and 10M excesses relative to the 1M excess sample. The degree of modification was greatest for the 6M and 10M excess at 60% and 95%, respectively. While a high degree of modification is desirable, a high DVS excess may cause the hydrogel to crosslink to other available vinyl sulfone groups on the HA backbone. This prevents vinyl sulfone groups from binding to target functional groups on bioactive and crosslinking agents. The 3M excess sample provides 40% degree of modification, which allows for biomolecular conjugation and crosslinking of hydrogel backbone. The HA treated with 3M excess of DVS was used to determine the ideal duration for the reaction. The samples were prepared at the following reaction times: 10 min, 15min, 20 min, 25 min, 30 min,

and 40 min. A statistical difference was observed between the 15 min and the longer reaction times. However, a significant difference was not observed for the degree of modification when the HA and DVS reacted for the 20 min, 25 min, 30 min, and 40 min (Fig. 3C.). Therefore, based upon this data, the 3M excess of DVS was used to react with HA for 20 min for further experimentation due to the optimal degree of modification and shortest reaction time.

Through confirmation of H-NMR and FTIR, it was determined that the HA backbone was successfully modified. The degree of modification is critical for the gelation of the HA hydrogel. As the degree of polymerization is controlled by the available functional groups, it is important to have substantial amount of vinyl sulfone groups to bind to the PEG-thiol in order to crosslink the hydrogel. Also, for neural engineering and other tissue engineering applications, the crosslinking of proteins, peptides, DNA aptamers, growth factors, and other bioactive agents to the backbone of the hydrogel scaffold is helpful to modulate apoptosis and other cellular processes. The modification using these bioactive agents can be conjugated to the acrylate group via Michael addition reaction. Therefore, having a significant amount of vinyl sulfone groups for crosslinking and conjugation of bioactive agent is critical.

Previous studies have demonstrated using various chemistries to modify the backbone of the HA with thiols, acrylates, vinyl sulfones, and amines, as well as crosslinking chemistry for hydrogel formation. Kim *et al*. reported using acrylated HA and a PEG-thiol; however, to acrylate the HA, a two-step reaction was required: (1) to add amine groups and (2) to acrylate the HA backbone[27]. The first reaction took 8 hrs and the solution had to be dialyzed to remove the unbound crosslinker prior to adding the acrylates, which required an additional 12 hrs to complete the fabrication process. Jin et al. also reported a lengthy multi-step Michael addition reaction using thiolated HA and VS-modified PEG. The authors reported a five step process for

the degradation and thiolation of the HA backbone, as well as for the fabrication of VS-modified PEG[36]. The advantage of our method is that it is a one-step reaction to functionalize the HA with vinyl sulfone groups, which occurs within 20 minutes. Also, the crosslinking step using the PEG-thiol occurs rapidly within 3-5 min, whereas other studies have reported gelation times on the order of hours. Earlier, Hoffman *et al.* fabricated crosslinked HA beads by uncontrolled reaction using DVS via Michael addition reaction[37]. Also, Ibrahim *et al*. fabricated HA hydrogels using HA or HA-oligomers and crosslinked using DVS. They used radical addition crosslinking between the hydroxyl groups on the HA and the vinyl groups provided by the DVS and reported a gelation time of 2 hrs[38]. Although both HA and DVS were used in our study and in the previously mentioned study, the differences are in the utilization of the functional groups; our system focuses on acrylates and thiols while other studies use hydroxyl and vinyl groups. Other methods to modify the HA backbone involved using carbodimide chemistry after introduction of amine groups to the backbone of HA[32], which also involves two-step reaction chemistry. Furthermore, the gelation time reported in previous studies is lengthy for *in situ* gelling neural applications. Organic solvents have also been used for the reaction[39]; however, denaturing the natural polymer may be an issue.

The functionalization of the HA developed in this study allows for conjugation of bioactive molecules in addition to crosslinking. Prestwich *et al*. is one of the first to report using HA as a hydrogel scaffold and modified the hydrogel to conjugate bioactive agents to the backbone[25]. The earlier protocols required crosslinking the hydrogel at pH in the acidic range of 3.5-4.75. As a scaffold, the pH is an important parameter to control if the application involves cell encapsulation and in vivo transplantation. The crosslinking of our HA solution with PEG-thiol occurs at physiologically relevant pH. The more recent protocols involved HA hydrogels

that were crosslinked using thiolated HA and PEGs with acrylate (diacrylate or dimethacrylate) or acrylamide groups (diamethacrylamide or diacrylamide)[40-42] . The studies demonstrated that gelation of the hydrogel with thiolated HA crosslinked with PEG-diacrylate occurred in 10 min; however, the other gels required up to several days[43]. In our study, y the HA backbone was modified with VS to allow for quick gelation time, and in addition, allow for bioactive agents, such as antibodies ,to be conjugated to the hydrogel for neural applications.

3.2. Characterization of HA Hydrogel

SEM was performed to visualize hydrogel porosity and size. In Figure 4, 0.75% HA hydrogel was crosslinked with various PEG-thiol percentages (1%. 5%, and 20% w/v) to examine the pore morphology and the interconnectivity of the scaffold. The hydrogels were indeed a porous structure pore diameter ranging from 5 μm to 100 μm. An increase in the percent PEG-thiol concentration corresponded to higher connectivity of HA and smaller pore size. The pore size of scaffolds is a critical parameter for neural applications due to the following: 1) diffusion of gas, nutrients, and proteins and growth factors, (2) cell migration/infiltration through and out of the scaffold, and (3) axonal outgrowth. The range of pore sizes within the HA hydrogel meets the requirements for all three of these parameters, indicating that the hydrogel is suitable for neural engineering applications.

Swelling and degradation studies were performed on the HA hydrogels in order to characterize the response of the samples within an aqueous environment, which is important for 3D cell culture and *in vivo* implantation. It is hypothesized that swelling and degradation would be affected by the crosslinking density as well as HA concentration. Therefore, samples with different percent weights of PEG-thiol and HA were prepared, as specified in the *materials and*

methods section. Figure 5A-C shows percent weight change of different hydrogel conditions over the initial 96 hr period. The HA hydrogel discs were weighed at 3 hrs, 6 hrs, 12 hrs, 24 hrs, 48 hrs, 72 hrs, and 96 hrs. Equilibrium was reached at the 24 hr time point in all conditions. A significant change in weight did not occur for the subsequent time points. At a constant HA percentage (0.75% w/v), an increase in the percentage of PEG-thiol (w/v) resulted in the increase of percent swelling of the hydrogel (Fig. 5A). Therefore, the HA gel crosslinked with 20% PEG-thiol had the highest degree of swelling and the gel with 1% PEG-thiol had the least. The increase in swelling observed may be attributed to the improved hydrophilicity provided by the PEG based crosslinker[44]. Furthermore, hydrogels crosslinked with 4-arm PEG-thiol have been shown to have increased swelling properties as PEG-spacer compounds increase hydrophilicity[45] The hydrogels crosslinked with 20% 4 arm PEG-thiol increased by 329%, whereas, gels crosslinked with 1% PEG-thiol increased to 217% relative to the initial time point. The swelling behavior in relation to the amount of crosslinking has been extensively studied[46] and the selected hydrogel substrate stiffness and swelling percent are important parameters for neuron cultures. While a significance was not observed, a clear variation in swelling data was seen in the graph between samples crosslinked with the lower PEG-thiol concentrations compared to the higher concentrations. As a large amount of swelling is not desirable for *in vivo* injection, the lower PEG-thiol percentage was selected for evaluating the effects of HA weight percent on hydrogel swelling characteristics. Subsequently, the percentage of PEG-thiol was kept constant at 1% and various percentage of HA was used, 0.5%, 0.75%, and 1% to determine how swelling was affected by the polymer concentration. As PEG-thiol and HA are both hydrophilic, it was expected that the 1% HA would swell the most, while the 0.5% sample would swell the least. However, a significant difference was not observed as seen in Figure 5B. Therefore, a change in

HA concentration did not affect the swelling. HA hydrogels of various volume ratios of HA to PEG-thiol were also tested to determine if the combined ratios of HA to PEG affected swelling characteristic. The hydrogels with the ratio of 3:1 and 7:1 of HA and PEG thiol had significantly greater percentage swelling, which increased to 232% and 238% compared to the original weight of the hydrogel, whereas the 1:1 ratio of HA to PEG-thiol swelled the least (Fig. 5C). Hydrophilic polymers, such as HA, swell significantly in water, thus the sample with the highest HA volume ratio would swell the most[47]. As the concentration and volume of PEG-thiol were held constant, the increase in swelling observed in figure 5 C is primarily due to the increase in HA volume present in the sample. The images of the 0.75% HA crosslinked with 1% PEG-thiol prior to swelling and after 24 hrs of swelling in both DDI H_2O and PBS can be seen in Figure 5D.

The nervous system has a very dynamic microenvironment after injury and during the progression of disease states. The glial cells release a variety of proteins, enzymes, and growth factors that are both promoting and inhibitory for repair, such as hyaluronidase. It is imperative that the scaffold be present during this time as to be able to support axonal outgrowth. As HA is naturally found in the body, it is important to characterize the enzymatic degradation of the HA hydrogel to ensure the presence and integrity of the scaffold. Thus, degradation studies were conducted to determine the hydrogel integrity. For the degradation studies, the hydrogels were allowed to swell for the first 24 hrs in PBS and then placed in PBS containing hyaluronidase (10 U/mL). The degradation study was performed with constant HA (0.75%) and PEG-thiol (1%) percentages, respectively (w/v) for 4 consecutive days. During the first 12 hours, the HA hydrogel discs swelled due to influx of the solvent (PBS) and its salt content. Due to the salt influx, the hyaluronidase was not added until equilibrium was reached. The weight of the

hydrogel plateaued at the 24 hr time point, and thus initial measurements were taken then followed by addition of the enzyme. The samples that were crosslinked due to the higher percent of PEG-thiol swelled the most compared to the 1% PEG-thiol as seen previously in the swelling experiment. For the following 72 hrs, the HA hydrogel degraded due to the enzyme. The final degradation percent for the 1%, 5%, and 15% PEG-thiol samples at the 96 hr time point were 17%, 11%, and 27%, respectively (Fig. 5E, left panel). The sample with the highest crosslinker concentration degraded the least. Despite the initial differences in swelling within the initial 24 hrs and the differences in the crosslinking density the degradation percent for all three samples was insignificant. The percentage of HA within each sample was then varied to observe the effects of polymer concentration on degradation. As a higher crosslinking concentration did not change the degradation, it is ideal to use a lower PEG-thiol concentration to minimize PEG induced cytoxicity in culture. For the conditions where the HA percentage (w/v) was varied and the PEG-thiol was kept constant, the 0.5% HA, 0.75% HA, and 1% HA hydrogels degraded to 13%, 19%, and 30% of its original weight; however, a significant difference was not observed among the conditions (Fig. 5E, right panel). The higher polymer concentration degraded the least due to a higher crosslinking density in the sample[36]. As can be seen in Figure 5E, the HA is still present at 4 days regardless of the degradation.

The effect of anti-Fas conjugated to the hydrogel on the swelling and degradation properties was also investigated using hydrogels at 0.75% HA and 1% PEG-thiol. Anti-Fas conjugated HA hydrogels showed reduced amount of swelling compared to the non-conjugated hydrogels (Fig, F, and left panel). This may be attributed to the presence of a large antibody within the nanoporous structure that contributes to reduced diffusion potential. While degradation is expected to be dependent on the amount of HA present, a difference was observed

in the degradation properties of the antibody conjugated hydrogels. As seen in Figure F, right panel, the anti-Fas HA hydrogel was less susceptible to enzyme degradation and maintained about 50% of its initial mass after 4 days. This may be due to the antibody conjugated to the polymer backbone, thus enhan[36]cing the rigidity of the hydrogel. Alternatively, the presence of the antibody within the polymer may alter the enzyme diffusion into the hydrogel making it less susceptible to degradation. Further, steric hindrance due to the presence of a large antibody may also alter enzyme-substrate interactions[48].

Lastly, to characterize the mechanical properties of the HA hydrogel, rheology was performed to determine the storage modulus of the various concentrations of HA crosslinked with different percentages of the PEG-thiol, as mechanical mismatch between the hydrogel scaffold and host tissue is undesirable. As demonstrated in Figure 6A, the 1% HA hydrogel had a storage modulus of approximately 350 Pa, whereas the 0.75% and 0.5% HA hydrogels had storage moduli of 247 Pa and 111 Pa, respectively. A statistical significance for the 0.5% and 0.75% HA samples compared to the gel crosslinked with 1% PEG-thiol was not observed, however the 1% HA sample was significant relative to the lowest HA concentration. There was an increasing trend in storage modulus as the HA concentration was increased. This is due to the proportional relationship between polymer concentration and mechanical strength seen in natural hydrogels[49, 50]. As the polymer chain density increases in the sample, there is an increase in the stiffness. Therefore, it is expected that the 1% HA hydrogel had the highest storage modulus. The moduli for the 0.75% and 0.5% HA hydrogels was similar to that of the central nervous system[51], and statistical significance did not exist between the conditions. Therefore, the 0.75% HA hydrogel was used when varying the percent concentration for the PEG-thiol. Previous literature has shown that varying the crosslinking density by increasing the concentration or

decreasing the molecular weight of PEG-thiol causes an increase in hydrogel stiffness[52]. In this experiment, PEG-thiol molecular weight was held constant, and only the concentration was varied. Figure 6B shows that the storage modulus of the hydrogel increased, as the percent (w/v) of PEG-thiol increased. The storage moduli were 246Pa, 124 Pa, 82 Pa, and 85 Pa for 20%, 15%, 5%, and 1% (w/v) of PEG-thiol, respectively. The 15% and 20% PEG-thiol crosslinked hydrogels were statistically greater than the 1% and 5% PEG-thiol samples. It has been shown that higher concentrations of PEG can be cytotoxic to cells[53, 54], thus it is not desirable to use a high PEG-thiol concentration. As the storage moduli for the 1% and 5% PEG-thiol were similar, the 1% PEG-thiol was chosen for the remaining cell viability experiments to minimize unwanted cytotoxic effects and not compromise the mechanical properties of the hydrogel. The storage moduli were obtained for various volume ratios of HA to PEG-thiol, 1:1, 3:1, and 7:1; a statistical difference was not observed (Fig. 6C). The mechanical properties, such as the storage moduli, of scaffolds used for neural engineering applications are critical. If the mechanical properties of the scaffold are significantly higher than the host tissue, then further damage can occur due to mechanical mismatch. Also, a scaffold that provides a similar microenvironment as the host tissue will be the most successful in promoting axonal outgrowth. Cell transplantation, especially NSC transplantation, is a promising therapeutic strategy for CNS repair. Therefore, it is advantageous that the HA hydrogel have a storage modulus similar to that of brains if utilizing the hydrogel for NSC transplantation.

An ideal HA: PEG-thiol concentration and ratio would be one that does not swell significantly, does not degrade during the dynamic time period after injury and has a modulus similar to nervous tissue. Therefore, the 0.75% HA and 1% PEG-thiol at a 1:1 ratio is ideal for the completion of future experiments.

3.3. Characterization of Cell Viability, Proliferation, and Neurite Length within Hydrogel Scaffold

After characterizing the HA hydrogel, experiments were performed to determine if the hydrogel was suitable for cellular applications. The rheological data demonstrated that the 0.75% HA and 1% PEG had a storage modulus that was similar to that of the nervous system tissue, as well as minimal swelling amongst the various hydrogel formulations; therefore, this was the concentration that was used for the cell viability, proliferation, and DRG neurite length studies. The CT-1005 were seeded within the HA hydrogel to characterize cell viability and proliferation potential. The Live/Dead assay was performed 24 hrs and 48 hrs post-seeding. The majority of the CT-1005 (green) are viable and only a few cells died indicating that the hydrogel is not inducing a cytotoxic response (Fig. 7A). Additionally, the positive Ki-67 staining indicates that the HA hydrogel supports the growth of these cells (Fig. 7B). As fibroblasts are found in the nervous system and have similar characteristics as supportive glial cells in the CNS, this is indicative that the glial cells will be viable in the hydrogel as well.

In addition, primary NSCs were cultured as single cells in the 0.75% HA and 1% PEG hydrogels for 24 hrs and 48 hrs. NSCs have become an important therapeutic strategy for CNS repair, as the NSCs can replenish the lost neuronal population. Therefore, the Live/Dead assay was performed to ensure that the NSCs are viable in the HA hydrogel. The majority of the NSCs were viable for 24 and 48 hrs time points. A minimal number of NSCs were observed to be positive for ethidium homodimer (Fig. 8A). Proliferation was also assessed in the NSCs with Ki-67, which were positively stained 48 hrs post-seeding (Fig. 8B). For neural engineering applications, viable and proliferative cells within the hydrogel are necessary to repair the tissue

after injury or disease. Although transplanting NSCs to replace the apoptotic neuronal population, as well as glia cells, has been an effective therapeutic strategy, it has been shown that less than 10% of the original cell graft remains viable[55, 56]. It has been demonstrated that the survival rate of the transplanted NSCs or progenitor cells increases significantly when implanted or embedded within the hydrogel[57-59]. Therefore, the use of hydrogels increases the survival rate of the transplanted NSCs. HA hydrogels are desirable as it is one of the main ECM proteins in the CNS and these cells have the receptors, CD44 (also known as RHAMM) and intercellular adhesion molecule-1 (ICAM-1) that bind to the HA. CD44 is a HA-mediated motility receptor[60, 61]; whereas ICAM-1 is a cell adhesion based receptor[62, 63]. These receptors and the HA receptor play a vital role in the migration and differentiation of the NSCs. For NSCs to differentiate into neurons, it is important the hydrogel scaffold provides the correct cues. With the NSCs having the receptors to bind to the HA hydrogel, they have the mechanism to interact with the scaffold, which allows for (1) migration of the cells and enhanced integration with the host tissue, and (2) differentiation of the NSCs into neurons.

The cell viability studies indicate that the HA hydrogel does support neuronal and non-neuronal cell types. In addition to culturing to ensure cell viability, whole E9 chick DRGs containing neurons and glial cells were cultured in the HA hydrogel to determine whether the hydrogel promoted neurite outgrowth as this is an important parameter for neural repair and engineering. Neurite extension was compared to 1% SeaPrep™ Agarose that has been previously reported to have robust outgrowth and used *in vivo* for peripheral and central nervous system repair[4, 64, 65]. After 48 hrs of culture, the DRGs were imaged and the neurite extension was measured. The DRGs have robust neurite extension into the HA hydrogel of approximately 900 μm in length, which was comparable to the neurite lengths grown in 1% SeaPrep™ Agarose

of 1000 μm average length (Fig. 9). Statistical difference was not observed between the two conditions. This demonstrates that our HA hydrogels support neurite outgrowth, which is a critical parameter for neural applications. The robust neurite outgrowth from the DRGs also signifies that the mechanical stiffness of the HA hydrogel is within the optimal range. If the mechanical stiffness is not conducive for DRG proliferation, than the neurites are not able to extend through the hydrogel[33, 66] and form connections as is needed for nerve repair.

3.4 Conjugation of Bioactive Molecule, Anti-Fas, to HA Hydrogel

To demonstrate the ability to conjugate bioactive molecules to our hydrogel, anti-Fas was conjugated to the HA backbone using available thiol groups on the antibody. The anti-Fas NMR spectrum has peaks between 3 and 4 ppm, which can be used to characterize conjugation of the molecule to HA (Fig. 10A). The anti-Fas NMR signature peak can be seen in the HA-Fas spectrum when compared to that of HA-VS (Fig. 10B). The degree of conjugation was characterized by quantifying the ratio of vinyl sulfone peaks between 6 -7 ppm and at 2 ppm relative to the HA-VS sample to show that the anti-Fas did bind to the target acrylate groups (Fig 10B). The degree of conjugation was calculated for HA samples conjugated with anti-Fas at different reaction time showing a 40% degree of conjugation at the given concentration, and was significant for all samples relative to the control HA–VS sample (Fig. 10C). This value was obtained by normalizing to the non-conjugated HA-VS sample. The reaction times tested were insignificant to the degree of conjugation. This demonstrates that our vinyl sulfone modified HA has the capability to bind to a thiolated bioactive molecule as well as binding to the crosslinker used, specifically PEG-thiol. As seen in Figure 11, anti-Fas HA forms a polymerized hydrogel after crosslinking with 1% PEG-thiol at a 1:1 ratio compared to the uncrosslinked sample after

15 minutes. We also used a photocrosslinker to polymerize the HA-VS and anti-Fas hydrogels showing the versatility of the chemistry used (data not shown). Following the confirmation from the NMR experiment that anti-Fas was conjugated to the HA backbone, cell viability experiments were performed to determine if anti-Fas induced apoptosis in the Jurkat and C8B4 cells, while protecting the NSCs. It is known that T-cells, macrophages, and NSCs respond to Fas due to the expression of the Fas receptor on their cell surface and anti-Fas has been shown to induce apoptosis in a T-cells and macrophages, while inducing proliferation in NSCs[67-70], after injury, T-cells and macrophages are recruited to the site of injury and promote apoptosis in the neural cells. T-cells infiltrate the site of injury within days, and their number increases in parallel to activation of the resident microglia, and recruitment of peripheral macrophages. Although the T-cell population is less than that of macrophages, they still promote tissue damage. While T-cells are present in the beginning phases of injury, macrophages remain the dominant inflammatory cells after injury. Macrophages are classified as pro-inflammatory (M1) or anti-inflammatory (M2) depending on their activation pathway[71]. Kigerl et al. has shown that M1 macrophages have a neurotoxic effect while M2 macrophages promote regenerative response despite the presence of inhibitor substrates within the site of CNS injury. After spinal cord injury, an M1 macrophage response is induced and overwhelms the minute M2 response, therefore reducing the M1 population is crucial to successful therapy[72]. C8B4 cells have been shown to express classic M1 markers, such as CD16/32, and Fas induced apoptosis of these cells would help promote an environment conducive for neural repair (data not shown). Thus, developing a hydrogel that can modulate the immune and inflammatory cell population after injury is crucial.

T-cells (Jurkat) and microglia (C8B4), cells were encapsulated and cultured in anti-Fas HA hydrogel to determine if apoptosis is induced. After 24 hrs, the encapsulated Jurkat cells in the anti-Fas conjugated HA were not viable as the majority of the cells are positive for ethidium homodimer (Fig. 12A). C8B4 cells were cultured in the anti-Fas conjugated hydrogel as well, and the majority of the cells were not viable as represented by the positive ethidium homodimer staining (Fig 12B). A few viable cells remain in the anti-Fas hydrogel, and that is due to differences in Fas expression compared to the Jurkat cells. The NSCs maintained viability in both the control HA hydrogel and anti-Fas HA thus demonstrating that the scaffold can support NSCs (Fig. 8A and 8C). The observed cellular responses to the anti-Fas HA hydrogel demonstrates that the antibody maintains its biological activity through the fabrication process and induces cell death in certain cell populations.

4. Conclusion

As presented in this paper, we have developed a fast, controllable one-step vinyl sulfone modification method using Michael addition reaction to fabricate rapidly polymerizing HA hydrogels that can be used for neural engineering applications. This highly tunable HA hydrogel allows for the degree of modification to be controlled based upon the molar excess of DVS, thus directly controlling mechanical properties. Also, functionalizing the HA backbone with vinyl sulfone groups allows for thiol-functionalized bioactive molecules to be conjugated directly to the scaffold, as well as crosslinking for polymerization. This modified HA hydrogel can be used as a scaffold to transplant cells, such as NSCs, as well as for filling a void space or gap to aid in repair after injury and promote axonal outgrowth.

Acknowledgments

We would like to thank Roshan James for his technical expertise with the rheological experiments, and Andrew Butler and Dr. Fotios Papadimitrakopoulos for their technical expertise with the H-NMR. We would also like to acknowledge Atieh Sadrei and Nicolas Rodriguez for their help in the DRG culturing and imaging. The data shown in the manuscript and the contents of the manuscript are views of the authors in entirety and not views of ACell Inc.

References

1. M. S. Shoichet, C. C. Tate, M. D. Baumann and M. C. LaPlaca, in *Indwelling Neural Implants: Strategies for Contending with the In Vivo Environment*, ed. W. M. Reichert, Boca Raton (FL), 2008.
2. R. Li, Z. Liu, Y. Pan, L. Chen, Z. Zhang and L. Lu, *Cell Biochem Biophys*, 2014, **68**, 449-454.
3. L. R. Robinson, *Suppl Clin Neurophysiol*, 2004, **57**, 173-186.
4. A. Jain, Y. T. Kim, R. J. McKeon and R. V. Bellamkonda, *Biomaterials*, 2006, **27**, 497-504.
5. R. Bellamkonda, J. P. Ranieri, N. Bouche and P. Aebischer, *J Biomed Mater Res*, 1995, **29**, 663-671.
6. G. P. Dillon, X. Yu, A. Sridharan, J. P. Ranieri and R. V. Bellamkonda, *J Biomater Sci Polym Ed*, 1998, **9**, 1049-1069.
7. J. P. Ranieri, R. Bellamkonda, E. J. Bekos, T. G. Vargo, J. A. Gardella, Jr. and P. Aebischer, *J Biomed Mater Res*, 1995, **29**, 779-785.
8. S. E. Stabenfeldt, A. J. Garcia and M. C. LaPlaca, *J Biomed Mater Res A*, 2006, **77**, 718-725.
9. S. M. O'Connor, D. A. Stenger, K. M. Shaffer, D. Maric, J. L. Barker and W. Ma, *J Neurosci Methods*, 2000, **102**, 187-195.
10. Y. Liang, P. Walczak and J. W. Bulte, *Biomaterials*, 2013, **34**, 5521-5529.
11. S. K. Seidlits, Z. Z. Khaing, R. R. Petersen, J. D. Nickels, J. E. Vanscoy, J. B. Shear and C. E. Schmidt, *Biomaterials*, 2010, **31**, 3930-3940.

12. S. Suri, L. H. Han, W. Zhang, A. Singh, S. Chen and C. E. Schmidt, *Biomed Microdevices*, 2011, **13**, 983-993.

13. M. J. Mahoney and K. S. Anseth, *Biomaterials*, 2006, **27**, 2265-2274.

14. A. Bignami, M. Hosley and D. Dahl, *Anat Embryol (Berl)*, 1993, **188**, 419-433.

15. B. Alberts, *Essential cell biology : an introduction to the molecular biology of the cell*, Garland Pub., New York, 1998.

16. C. B. Knudson and W. Knudson, *Semin Cell Dev Biol*, 2001, **12**, 69-78.

17. P. Ghosh, *Clin Exp Rheumatol*, 1994, **12**, 75-82.

18. B. V. Slaughter, S. S. Khurshid, O. Z. Fisher, A. Khademhosseini and N. A. Peppas, *Adv Mater*, 2009, **21**, 3307-3329.

19. M. R. M. E. Aguilar, C.,Gallardo, A., Vasquez, B., Roman, J.S., in *Topics in Tissue Engineering*, ed. N. Ashammakhi, Reis, R.L., Chiellini, E. , University of Oulu, Finland, vol. 3, ch. 6, pp. 2-27.

20. J. Park, E. Lim, S. Back, H. Na, Y. Park and K. Sun, *J Biomed Mater Res A*, 2010, **93**, 1091-1099.

21. Y. D. Park, N. Tirelli and J. A. Hubbell, *Biomaterials*, 2003, **24**, 893-900.

22. J. B. Leach, K. A. Bivens, C. N. Collins and C. E. Schmidt, *J Biomed Mater Res A*, 2004, **70**, 74-82.

23. P. Ducheyne, K. Healy, D. E. Hutmacher, D. W. Grainger and C. J. Kirkpatrick, *Comprehensive Biomaterials: Online Version*, Elsevier, 2011.

24. X. Q. Jia, J. A. Burdick, J. Kobler, R. J. Clifton, J. J. Rosowski, S. M. Zeitels and R. Langer, *Macromolecules*, 2004, **37**, 3239-3248.

25. G. D. Prestwich, D. M. Marecak, J. F. Marecek, K. P. Vercruysse and M. R. Ziebell, *J Control Release*, 1998, **53**, 93-103.

26. H. Tan, C. M. Ramirez, N. Miljkovic, H. Li, J. P. Rubin and K. G. Marra, *Biomaterials*, 2009, **30**, 6844-6853.

27. J. Kim, I. S. Kim, T. H. Cho, K. B. Lee, S. J. Hwang, G. Tae, I. Noh, S. H. Lee, Y. Park and K. Sun, *Biomaterials*, 2007, **28**, 1830-1837.

28. Y. Yu and Y. Chau, *Biomacromolecules*, 2012, **13**, 937-942.

29. H. Tan, A. J. DeFail, J. P. Rubin, C. R. Chu and K. G. Marra, *Journal of Biomedical Materials Research Part A*, 2010, **92**, 979-987.

30. O. Jeon, K. H. Bouhadir, J. M. Mansour and E. Alsberg, *Biomaterials*, 2009, **30**, 2724-2734.

31. F. Delben, R. Lapasin and S. Pricl, *Int J Biol Macromol*, 1990, **12**, 9-13.

32. J. A. Burdick, C. Chung, X. Jia, M. A. Randolph and R. Langer, *Biomacromolecules*, 2005, **6**, 386-391.

33. X. Yu and R. V. Bellamkonda, *J Neurosci Res*, 2001, **66**, 303-310.

34. F. Donghui, W. Beibei, X. Zheng and G. Qisheng, *Journal of Wuhan University of Technology-Mater. Sci. Ed.*, 2006, **21**, 32-34.

35. M. W. Ellzy, J. O. Jensen and J. G. Kay, *Spectrochimica Acta Part A: Molecular and Biomolecular Spectroscopy*, 2003, **59**, 867-881.

36. R. Jin, L. M. Teixeira, A. Krouwels, P. Dijkstra, C. Van Blitterswijk, M. Karperien and J. Feijen, *Acta Biomaterialia*, 2010, **6**, 1968-1977.

37. S. K. Hahn, S. Jelacic, R. V. Maier, P. S. Stayton and A. S. Hoffman, *Journal of Biomaterials Science, Polymer Edition*, 2004, **15**, 1111-1119.

38. S. Ibrahim, Q. K. Kang and A. Ramamurthi, *J Biomed Mater Res A*, 2010, **94**, 355-370.

39. S. A. Zawko, S. Suri, Q. Truong and C. E. Schmidt, *Acta Biomater*, 2009, **5**, 14-22.

40. T. Takezawa, *Nature Biotechnology*, 1990, **8**, 854.

41. G. A. Weng L, Wu Y, Chen W. , *Biomaterials*, 2008, **29**.

42. H. Yoon, Koo, H., Choi, KY., Chan Kwon, I, Choi, K. Park, JH., Kim, K, *Biomaterials*, 2013, **34**, 5273-5280.

43. X. Z. Shu, Y. Liu, F. Palumbo and G. D. Prestwich, *Biomaterials*, 2003, **24**, 3825-3834.

44. G. Lin, X. Zhang, S. R. Kumar and J. E. Mark, *Silicon*, 2009, **1**, 173-181.

45. G. T. Hermanson, *Bioconjugate techniques*, Academic press, 2013.

46. M. N. Collins and C. Birkinshaw, *Journal of Applied Polymer Science*, 2008, **109**, 923-931.

47. N. B. Ferapontov, M. G. Tokmachev, A. N. Gagarin, N. L. Strusovskaya and S. N. Khudyakova, *Reactive and Functional Polymers*, 2013, **73**, 1137-1143.

48. D. Dikovsky, H. Bianco-Peled and D. Seliktar, *Advanced Engineering Materials*, 2010, **12**, B200-B209.

49. C. K. Kuo and P. X. Ma, *Biomaterials*, 2001, **22**, 511-521.

50. B. L. Vernon, *Injectable Biomaterials: Science and Applications*, 2011.

51. Y. B. Lu, K. Franze, G. Seifert, C. Steinhauser, F. Kirchhoff, H. Wolburg, J. Guck, P. Janmey, E. Q. Wei, J. Kas and A. Reichenbach, *Proc Natl Acad Sci U S A*, 2006, **103**, 17759-17764.

52. S. Lee, X. Tong and F. Yang, *Acta biomaterialia*, 2014, **10**, 4167-4174.

53. R. Webster, V. Elliott, B. K. Park, D. Walker, M. Hankin and P. Taupin, in *PEGylated Protein Drugs: Basic Science and Clinical Applications*, ed. F. Veronese, Birkhäuser Basel, 2009, DOI: 10.1007/978-3-7643-8679-5_8, ch. 8, pp. 127-146.

54. O. Biondi, S. Motta and P. Mosesso, *Mutagenesis*, 2002, **17**, 261-264.

55. A. Bakshi, C. A. Keck, V. S. Koshkin, D. G. LeBold, R. Siman, E. Y. Snyder and T. K. McIntosh, *Brain Res*, 2005, **1065**, 8-19.

56. T. Kallur, V. Darsalia, O. Lindvall and Z. Kokaia, *J Neurosci Res*, 2006, **84**, 1630-1644.

57. L. Little, K. E. Healy and D. Schaffer, *Chem Rev*, 2008, **108**, 1787-1796.

58. D. R. Nisbet, D. Moses, T. R. Gengenbach, J. S. Forsythe, D. I. Finkelstein and M. K. Horne, *J Biomed Mater Res A*, 2009, **89**, 24-35.

59. M. J. Cooke, T. Zahir, S. R. Phillips, D. S. Shah, D. Athey, J. H. Lakey, M. S. Shoichet and S. A. Przyborski, *J Biomed Mater Res A*, 2010, **93**, 824-832.

60. C. M. Isacke and H. Yarwood, *The international journal of biochemistry & cell biology*, 2002, **34**, 718-721.

61. H. Zhu, N. Mitsuhashi, A. Klein, L. W. Barsky, K. Weinberg, M. L. Barr, A. Demetriou and G. D. Wu, *Stem Cells*, 2006, **24**, 928-935.

62. P. McCourt, B. Ek, N. Forsberg and S. Gustafson, *Journal of Biological Chemistry*, 1994, **269**, 30081-30084.

63. J. Entwistle, C. L. Hall and E. A. Turley, *Journal of cellular biochemistry*, 1996, **61**, 569-577.

64. M. C. Dodla and R. V. Bellamkonda, *Biomaterials*, 2008, **29**, 33-46.

65. X. Yu and R. V. Bellamkonda, *Tissue Eng*, 2003, **9**, 421-430.

66. A. P. Balgude, X. Yu, A. Szymanski and R. V. Bellamkonda, *Biomaterials*, 2001, **22**, 1077-1084.

67. S. C. W. Ko, Johnson, V.L., Chow, S.C., *Biochemical and Biophysical Research Communications*, 2000, **270**, 1009-1015.

68. M. Muschen, Moers C., and Beckmann, MW, *Immunology*, 2000, **99**, 69-77.

69. N. S. Corsini, I. Sancho-Martinez, S. Laudenklos, D. Glagow, S. Kumar, E. Letellier, P. Koch, M. Teodorczyk, S. Kleber and S. Klussmann, *Cell Stem Cell*, 2009, **5**, 178-190.

70. B. C. Richardson, N. D. Lalwani, K. J. Johnson and R. M. Marks, *European journal of immunology*, 1994, **24**, 2640-2645.

71. F. O. Martinez and S. Gordon, *F1000prime reports*, 2014, **6**.

72. K. A. Kigerl, J. C. Gensel, D. P. Ankeny, J. K. Alexander, D. J. Donnelly and P. G. Popovich, *The Journal of Neuroscience*, 2009, **29**, 13435-13444.

Figure Captions

Figure 1. Schematic showing modification of HA with DVS, conjugation, and chemical crosslinking. A one-step Michael addition reaction to functionalize the HA backbone with DVS was performed. **(A)** Reaction between HA and DVS to add vinyl sulfone groups to HA backbone at basic pH condition. To crosslink the HA to form a hydrogel, PEG-thiol was used to bind to the vinyl sulfone groups. **(B)** Biomolecule conjugation to the HA-VS sample and chemical crosslinking using the PEG-thiol to form a hydrogel.

Figure 2. FTIR spectrum confirmed DVS modification of HA backbone. FTIR spectrum for HA only, DVS only, and HA reacted with 3M excess of DVS (HA-VS) **(A)** The top spectrum is for HA only. Peak 1= 3275, Peak 2= 1607, Peak 3= 1405, Peak 4= 1037, Peak 5= 947, Peak 6= 604. **(B)** The second spectrum is for DVS. Peak 1= 3058, Peak 2= 1610, Peak 3= 1384, Peak 4= 1307, Peak 5= 1249, Peak 6= 1126, Peak 7= 973, Peak 8= 770, Peak 9= 714, Peak 10= 653, Peak 11= 596. **(C)** The third spectrum is the HA-VS. Peak 1= 3369, Peak 2= 1729, Peak 3= 1637, Peak 4= 1521, Peak 6= 1375, Peak 7= 1311, Peak 8= 1039. The peak at 1521 represents the vinyl sulfone group on the HA, thereby confirming that the HA has reacted with the DVS.

Figure 3. Confirmation of VS functionalization of HA using H-NMR and quantification of degree of a modification. **(A)** H-NMR spectrum for HA only and HA reacted with 3M excess of DVS (HA-VS). The peaks can be seen between 6.4 and 6.9 ppm in the HA-VS hydrogels (Peaks 1-3). This confirms the addition of vinyl sulfone through a one-step Michael addition reaction,. **(B)** The degree of modification was calculated by integrating the peaks for the vinyl sulfone

groups as described in the methods section for various molar excess of DVS. The 6M and 10M had the greatest degree of modification **(C)** In addition, various reaction times between the HA and DVS were tested for degree of modification. The 20 minute reaction time was statistically insignificant relative to the longer reaction times, and is the fastest time for functionalizing the HA backbone for the 3M DVS excess condition. **(B)** and **(C)** Letters represent significant difference of $p<0.05$ between indicated conditions.

Figure 4. SEM images of the hydrogel scaffold showing pore size and structure. **(A)** SEM image of the 0.75% HA hydrogel crosslinked with 1% PEG-thiol showing that the pore size is between 5 to 100 μm (500X). **(B)** SEM image of the 0.75% HA sample crosslinked with 5% PEG-thiol (500X). **(C)** SEM image of the 0.75% HA sample crosslinked with 20% PEG-thiol (500X).

Figure 5: Swelling and degradation of HA hydrogels. **(A)** HA hydrogel discs made with 0.75% HA and varied percentages (w/v) of PEG-thiol were used for crosslinking. The hydrogel discs were allowed to swell in DDI H_2O for 4 consecutive days. The sample crosslinked with 20% PEG-thiol had the highest degree of swelling as it was capable of holding more water **(B)** The discs were of 0.5%, 0.75% or 1% HA and crosslinked with 1% PEG-thiol (PEG-SH). Equilibrium was reached after 24 hours. The different HA percentages were insignificant to swelling properties. **(C)** Hydrogels with 0.75% HA and 1%PEG-SH were tested at different ratios to determine effect of HA content on degree of swelling. The sample with the highest HA content swelled the most, but was not statistically significant to the other samples. **(D)** Optical

images of the hydrogel pre-swelling and post-swelling using DDI H_2O and PBS. **(E)** The hydrogel discs were allowed to swell for the first 24 hrs in PBS and then the HA hydrogel was degraded using hyaluronidase for the following 72 hrs. The hydrogel swelled within the first 12 hrs and equilibrated by the 24 hrs time point. During the subsequent 72 hrs, a significant decrease in weight was observed. The degradation of the HA hydrogel with varied PEG-thiol can be seen in the left panel. The right panel depicts the graph for the degradation of when the percentage of HA is varied and the PEG-thiol is constant. **(F)** The swelling and degradation properties of anti-Fas conjugated HA hydrogel discs at 0.75% w/v and 1% PEG-thiol were compared to HA hydrogel. The protein conjugated hydrogel swelled more compared the HA hydrogel. Anti-Fas conjugated hydrogel degraded less than the non-conjugated control.

Figure 6: Storage moduli of HA hydrogel with varying HA and PEG concentrations. **(A)** Storage modulus of HA hydrogel with various HA percentages crosslinked with 20% PEG-thiol. The storage modulus for the 0.5% HA crosslinked with 1% PEG-thiol was significantly lower compared to the 1% HA. * $p<0.05$ compared to 1% HA. **(B)** Storage modulus values using 0.75% HA and various percentages of PEG-thiol. The 0.75% HA crosslinked with either 1% or 5% PEG thiol had similar storage moduli and were statistically lower than the hydrogels crosslinked using 20% PEG-thiol. $P<0.05$ compared to 20% PEG-thiol. **(A)** and **(B)** Letters represent significant difference of $p<0.05$ between indicated conditions. **(C)** A statistical difference was not observed for the storage moduli of HA hydrogel with various volume ratios of 0.75% HA to 1% 4-arm PEG thiol.

Figure 7: Viability of primary dermal fibroblasts in 1:1 HA hydrogel. **(A)** Live/Dead assay was performed 24 and 48 hours after seeding. Fluorescent images can be seen with Calcein positive staining in green, and Ethidium positive staining in red. The images in top row indicate that the majority of fibroblasts are viable. The images in the bottom row show that minimal cells are not viable. **(B)** Ki67 proliferative marker (green) indicates that fibroblasts retain proliferative capacity for up to 48 hours in the HA hydrogels.

Figure 8: Viable NSCs in 1:1 0.75% HA hydrogels: 1% PEG-SH. Cells cultured were viable at 24 hrs and 48 hrs time points. **(A)** Live/Dead assay was performed 24 and 48 hours after seeding. Fluorescent images can be seen with Calcein positive staining in green, and Ethidium positive staining in red. The images in the top row indicate that the majority of NSCs are viable. The images in the bottom row show that minimal cells are ethidium positive. **(B)** Ki67 proliferative marker (green) indicates that NSCs retain proliferative capacity for up to 48 hours in the HA hydrogels. **(C)** Anti-Fas conjugated HA hydrogel promotes NSC viability. NSCs were cultured in the HA and anti-Fas HA hydrogels for 24 hrs. Live/Dead assay was performed to determine NSC viability. It can be seen that in the HA hydrogel, the NSCs remain viable in both hydrogels (green); with minimal non-viable cells (red).

Figure 9. DRG neurite extension in HA and agarose hydrogels are comparable. DRGs were cultured in both agarose and HA hydrogels for 48 hrs. **(A)** Bright field images of DRG and neurites in 1% Agarose. **(B)** Bright field image of DRG and neurites in 3:1 of 0.75% HA

hydrogel. **(C)** Quantification of neurite outgrowth length in both hydrogels demonstrates that the neurite extension is similar and not statistically different.

Figure 10: 1H-NMR and Protein Conjugation to HA backbone. **(A)** The characteristic peaks for soluble anti-Fas are located between 3 and 4 ppm. **(B)** Comparison of pure HA and HA-VS shows appearance of characteristic DVS peaks between 6 and 7 ppm. The characteristic anti-Fas peaks appear in the anti-Fas HA hydrogel between 3 and 4 ppm. **(C)** The vinyl sulfone (Peaks 1-3) and HA peaks (4) were used to quantify anti-Fas conjugation There is a reduction in the ratio of the vinyl sulfone groups after conjugation of anti-Fas indicating that there is binding of the bioactive agent. Letters represent significant difference of $p<0.05$ between indicated conditions.

Figure 11: Crosslinking of anti-Fas HA with PEG-thiol. Crosslinking of the anti-Fas conjugated hydrogel precursor with PEG-thiol indicates that there is sufficient vinyl sulfone groups available for hydrogel polymerization.

Figure 12. Anti-Fas conjugated HA hydrogel induces T-cell and microglia cell death. T-cells and microglia were cultured in the HA and anti-Fas HA hydrogels for 24 hrs. Live/Dead assay was performed to determine T-cell viability. **(A)** It can be seen that in the HA hydrogel, the T-cells maintain viability in HA only hydrogel (green); however, the majority of the T-cells are dead in the anti-Fas conjugated HA hydrogels (red). **(B)** In the control hydrogel, microglia

remain viable (green) with minimal non-viable cells (red). The cells in the anti-Fas HA are predominately non-viable (red), with some viable cells present (green).

Figure 1

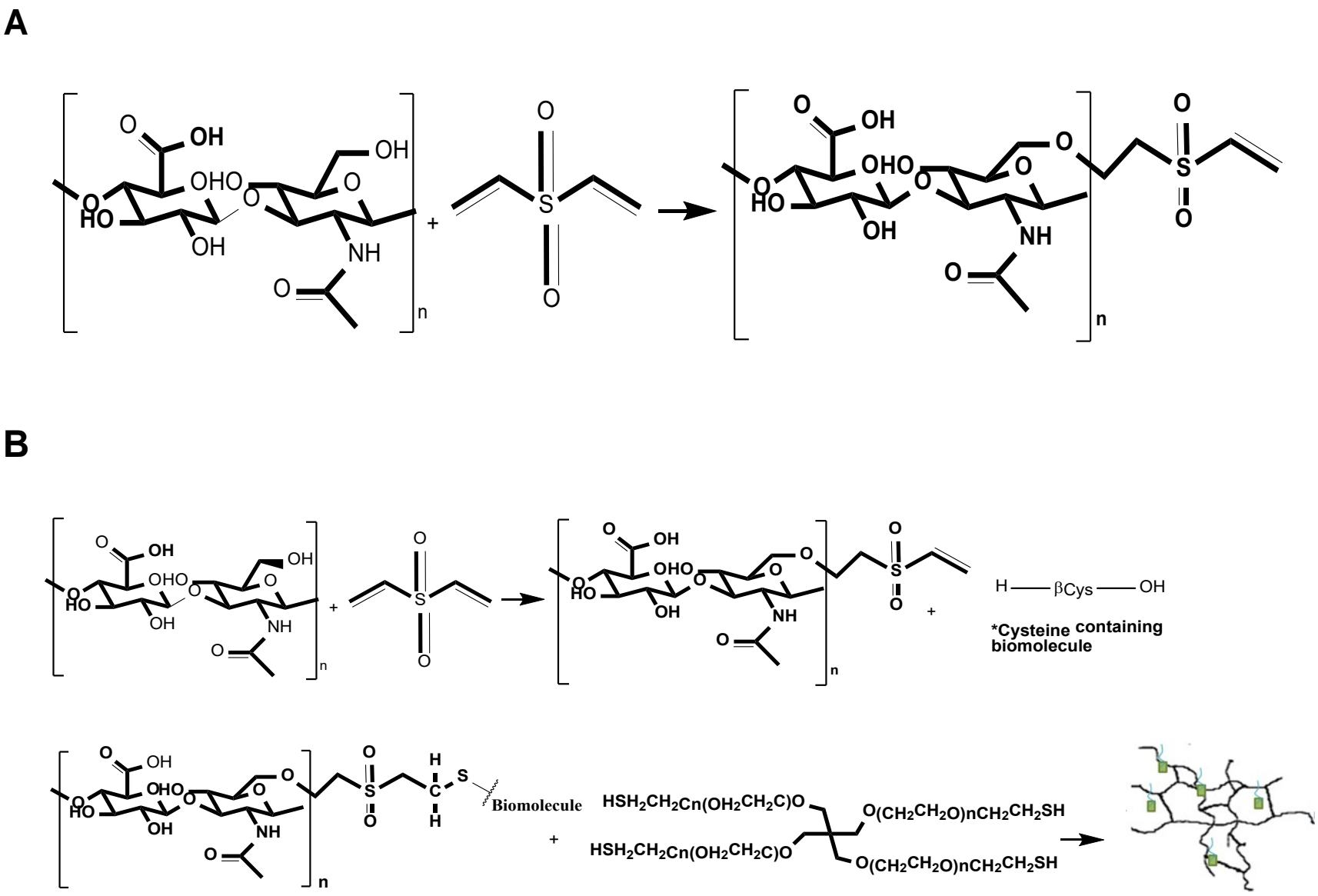

A

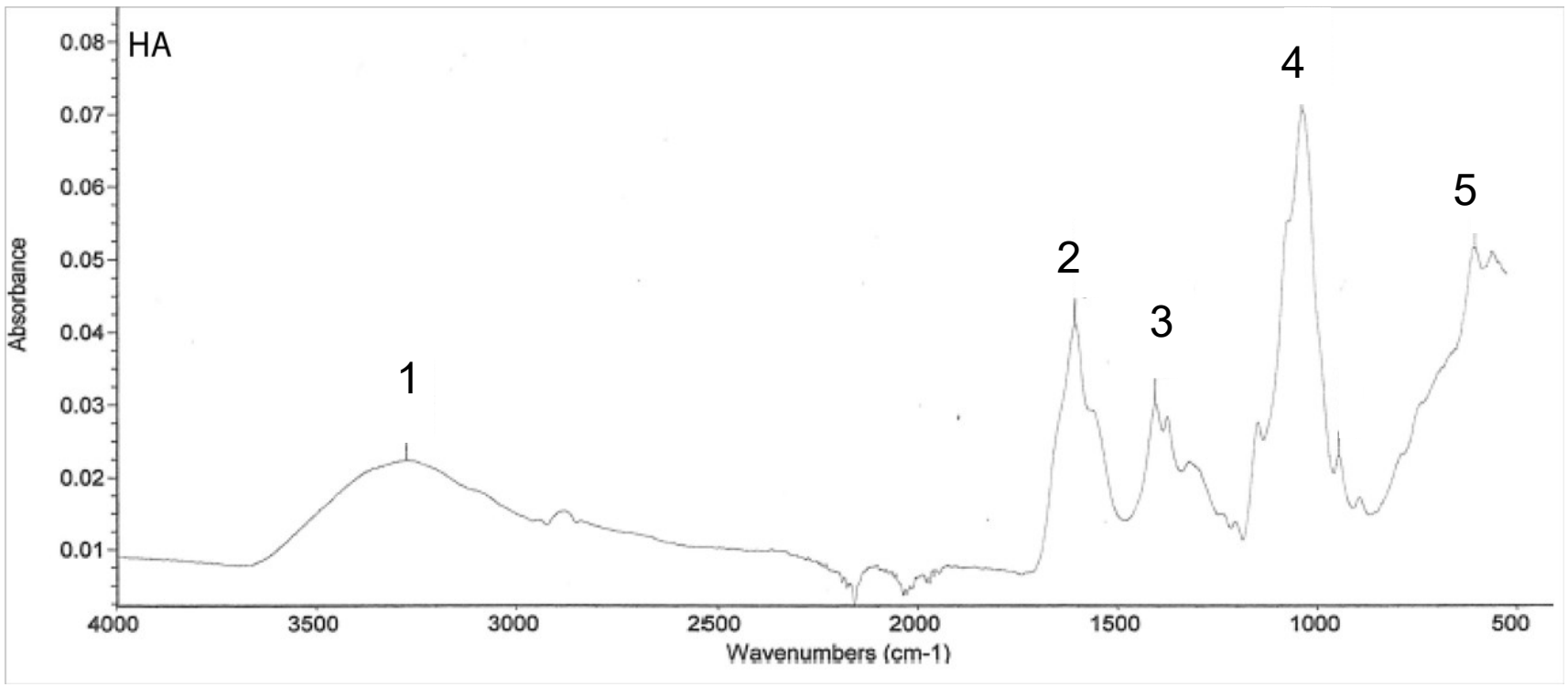

B

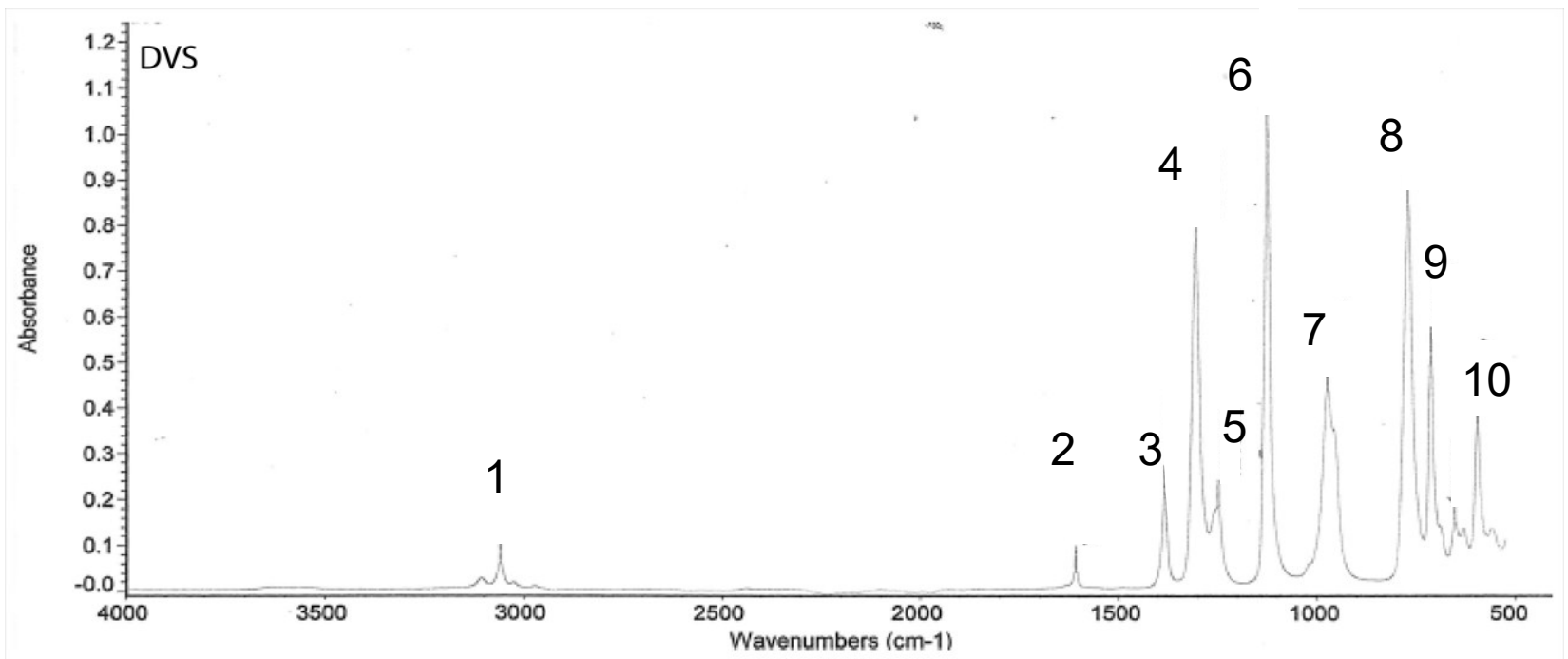

C

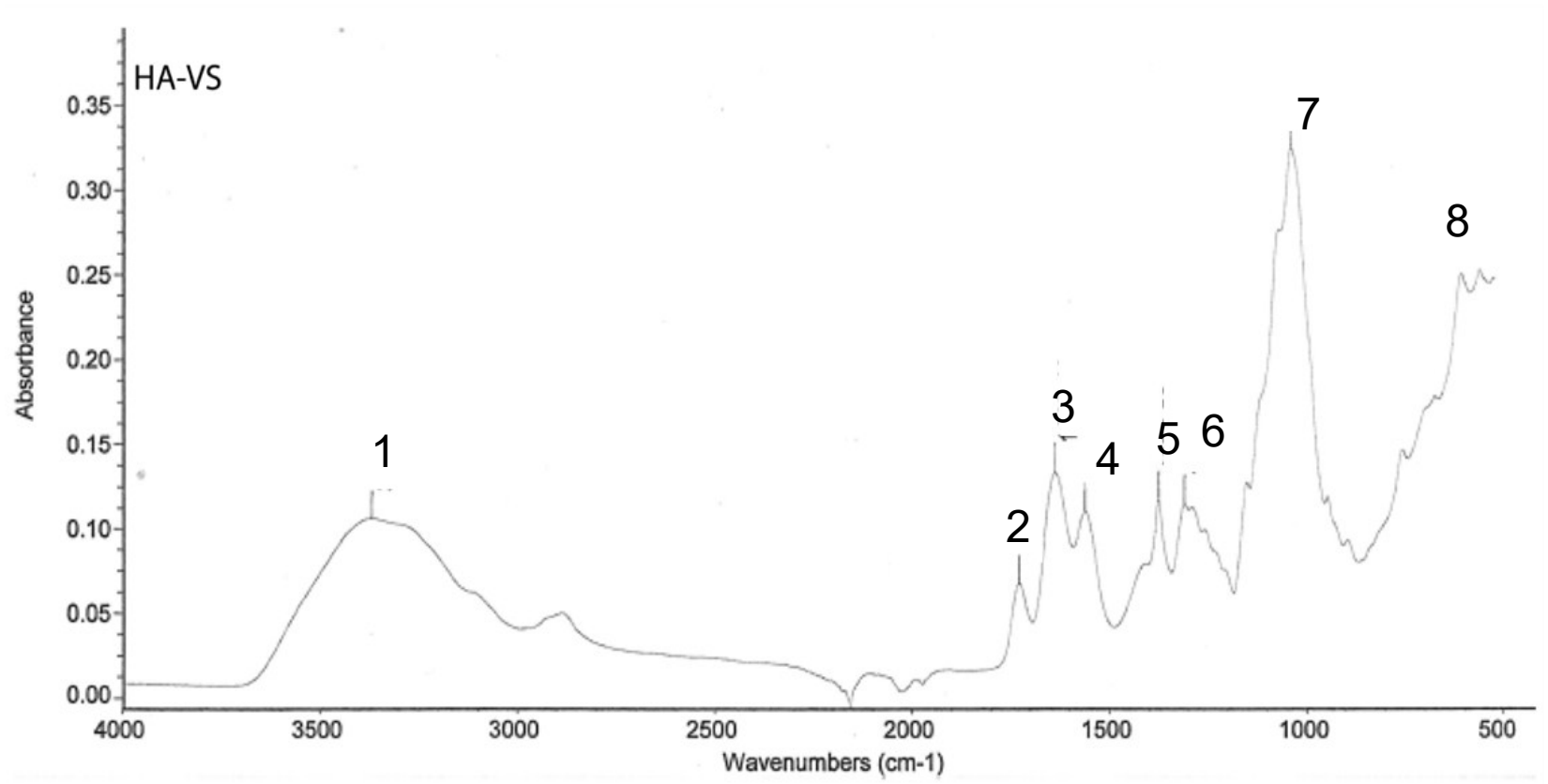

Figure 3

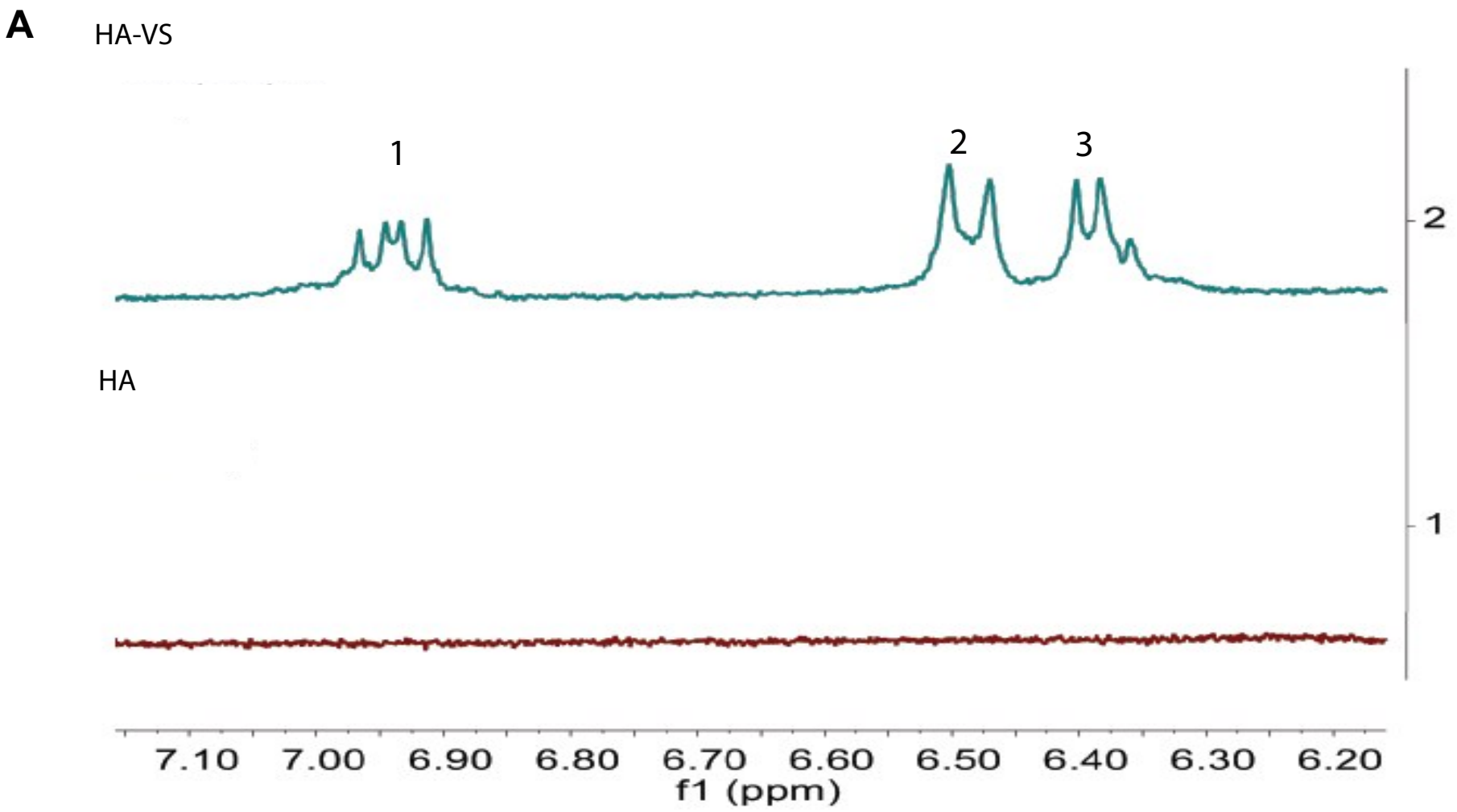

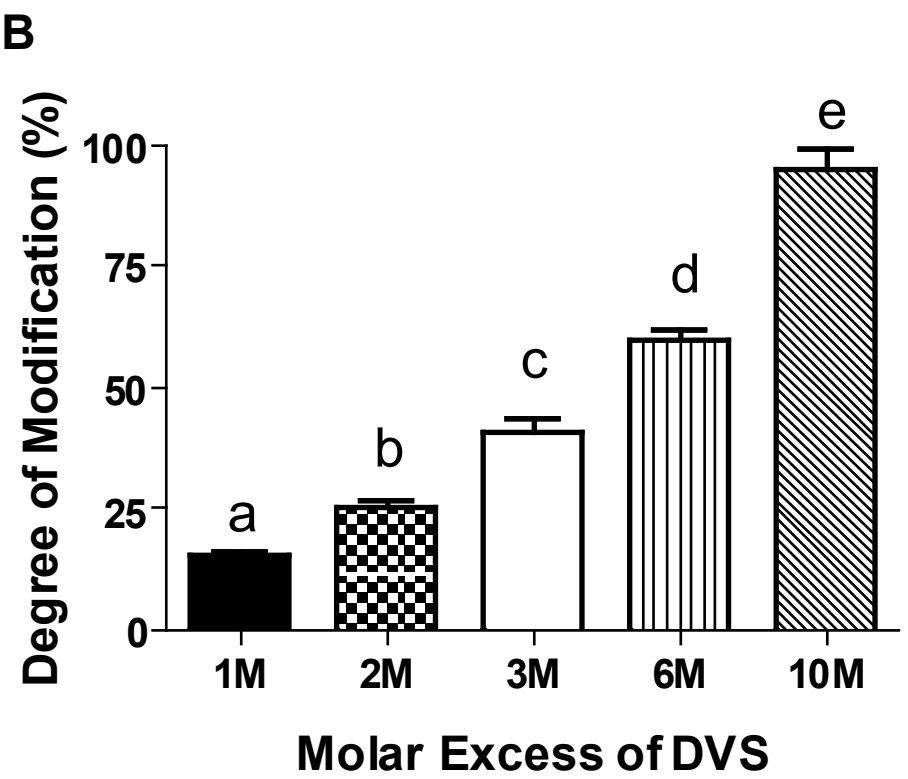

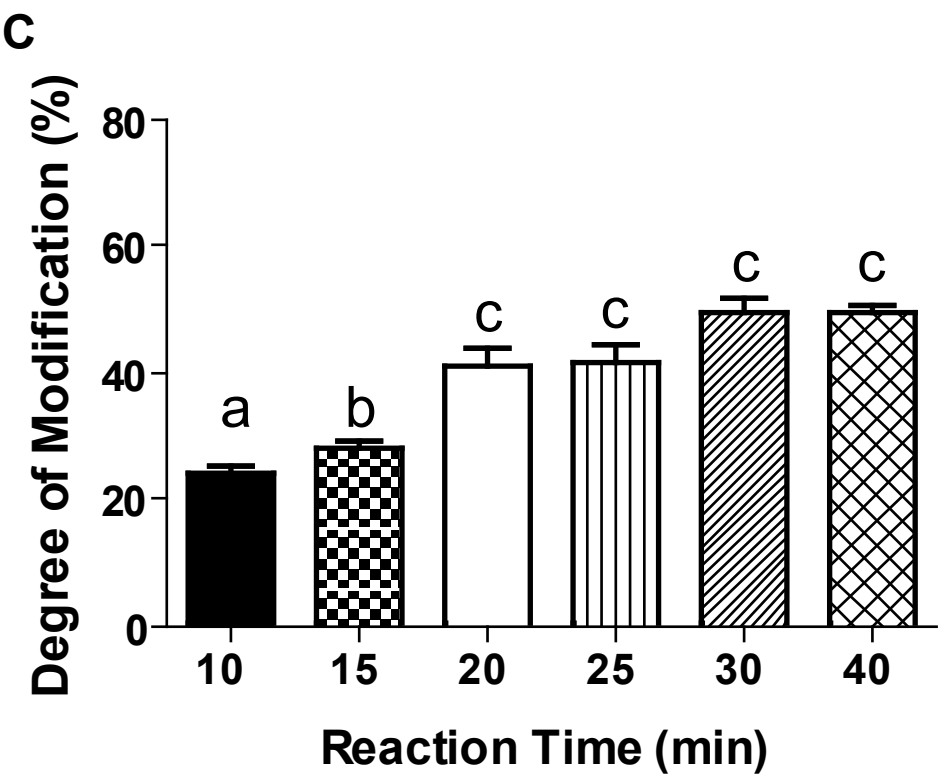

A

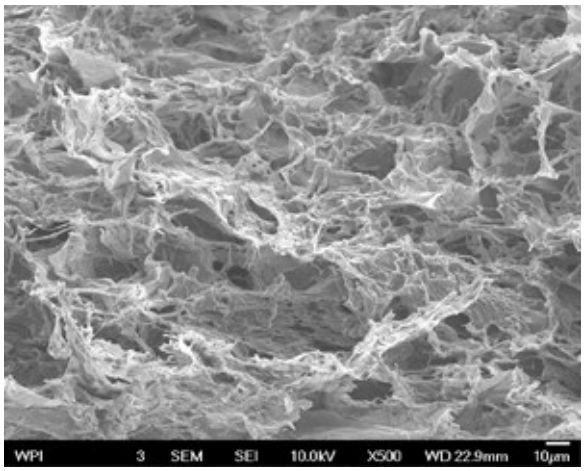

B

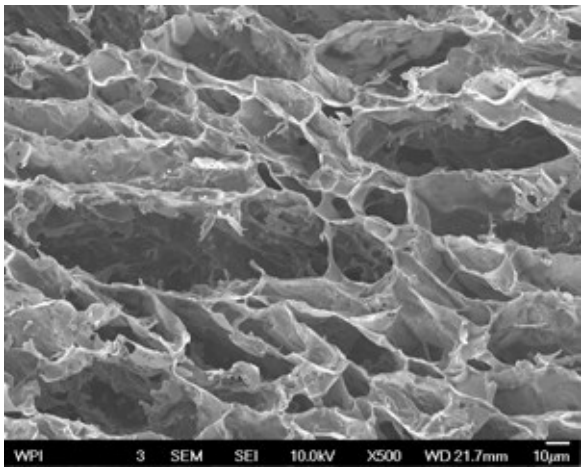

C

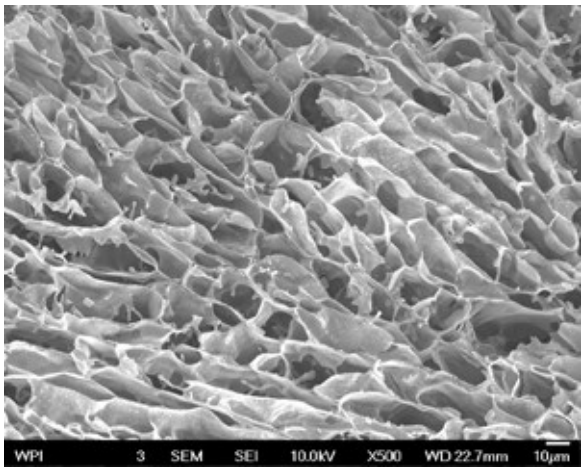

Figure 5

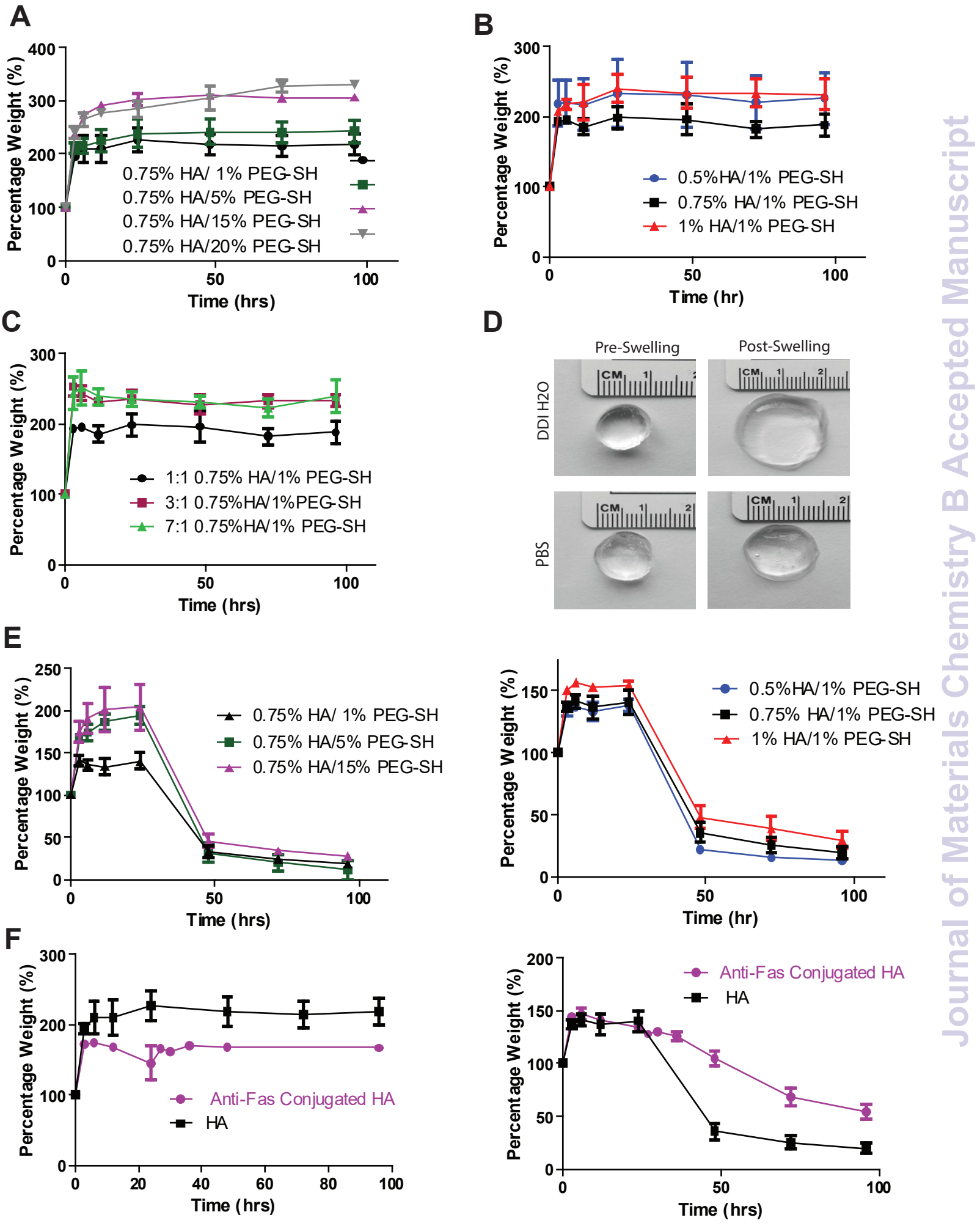

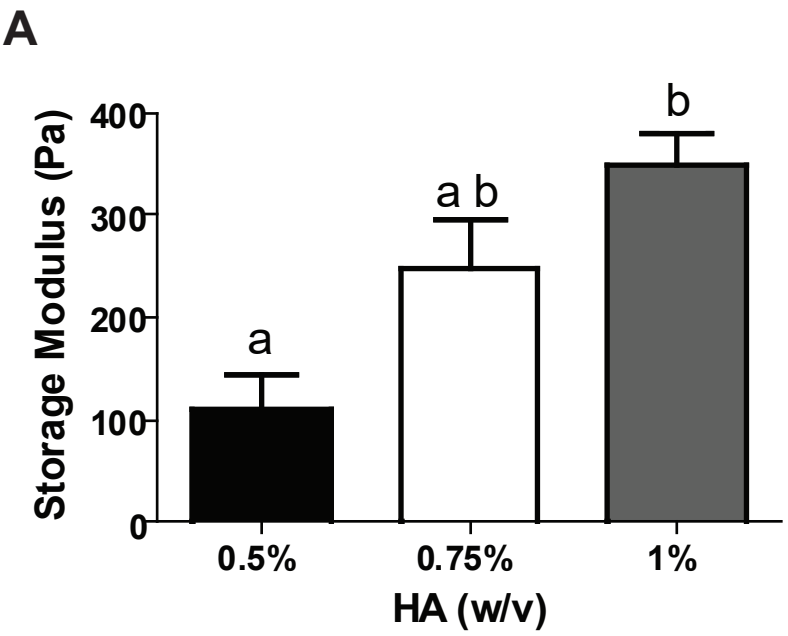

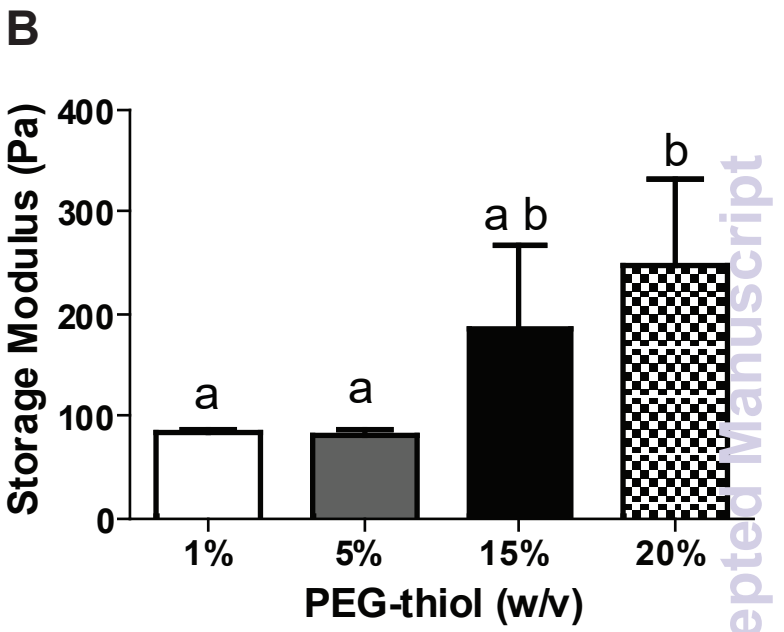

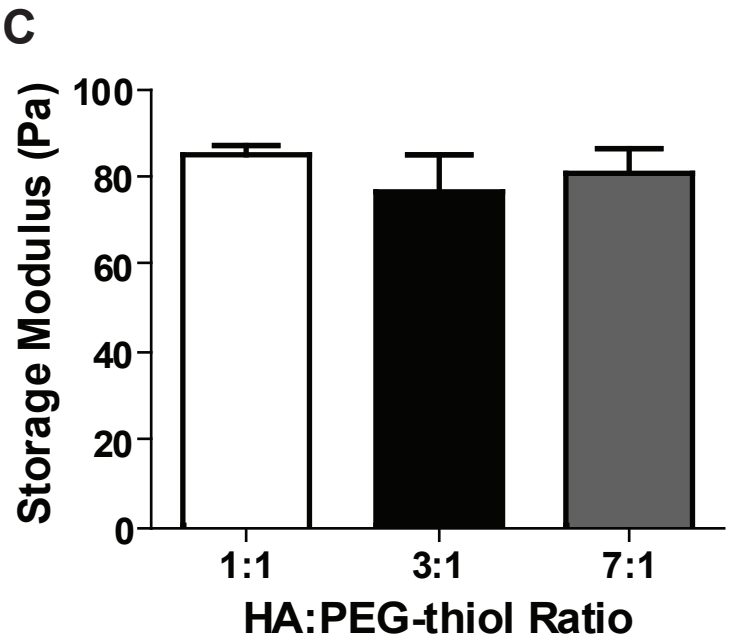

Figure 7

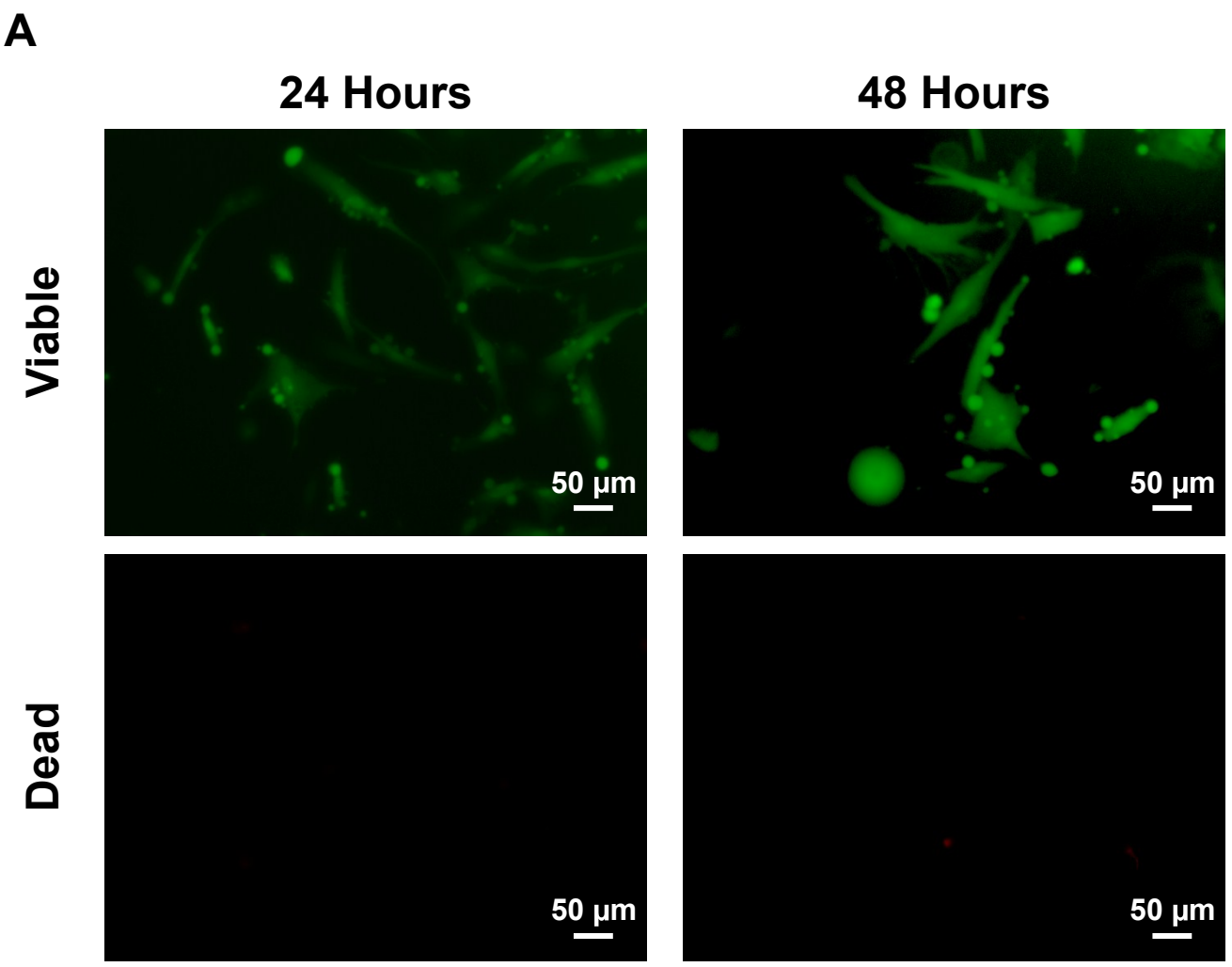

Figure 8

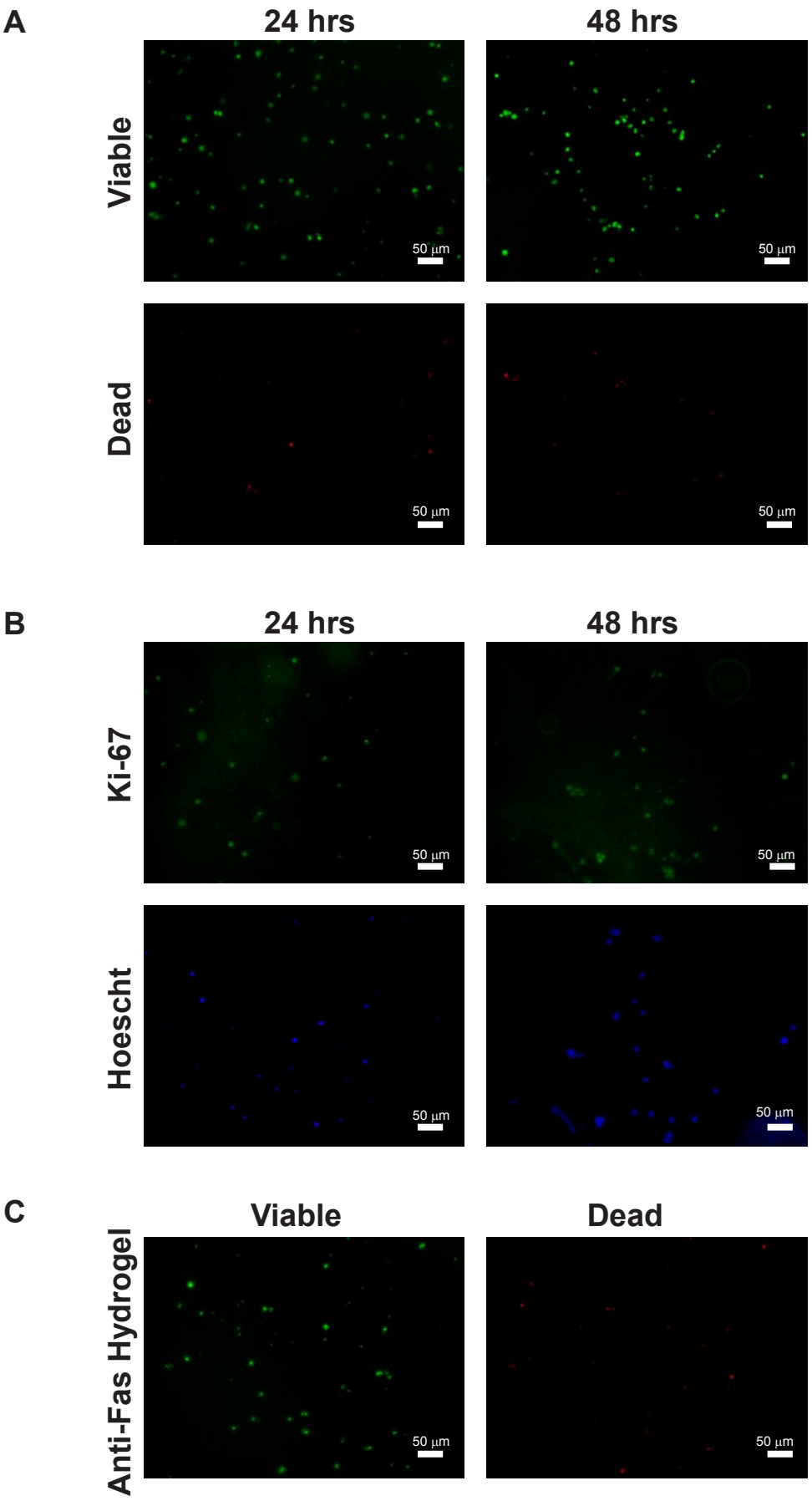

Figure 9

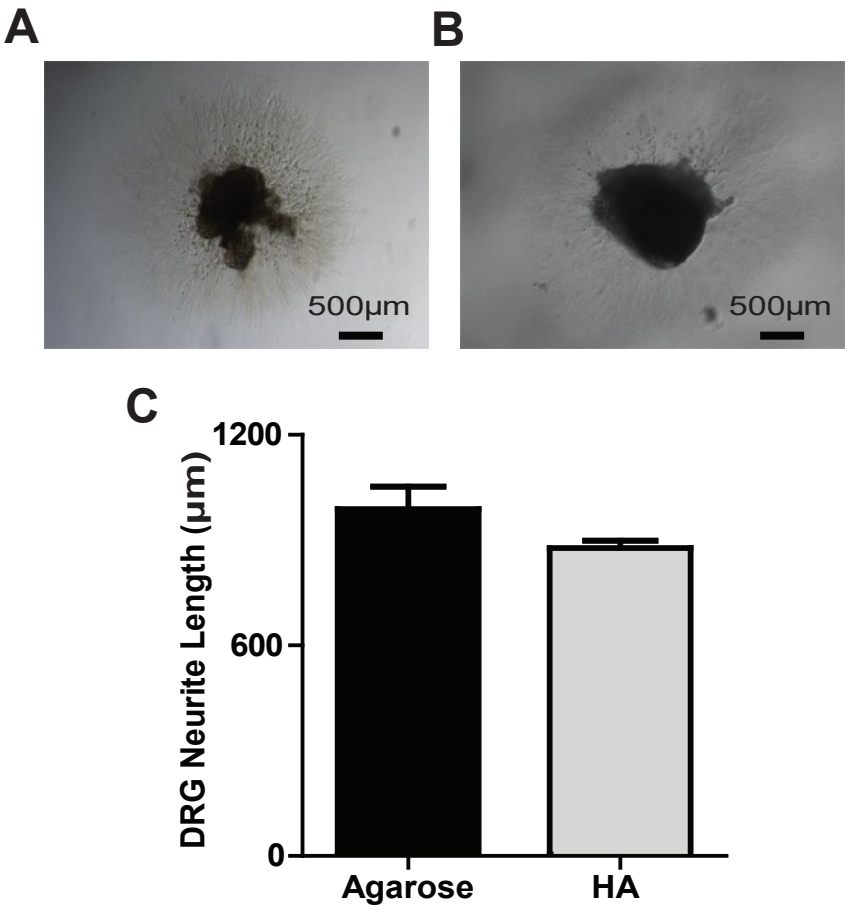

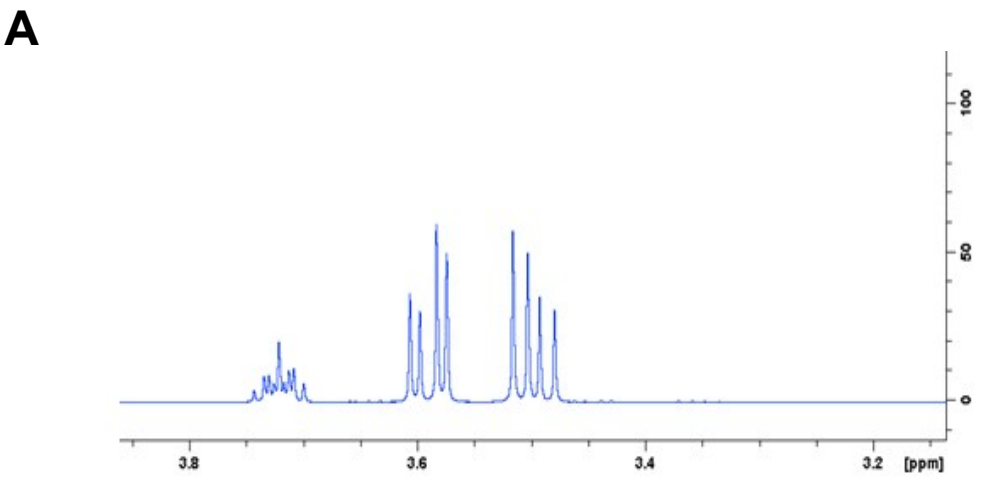

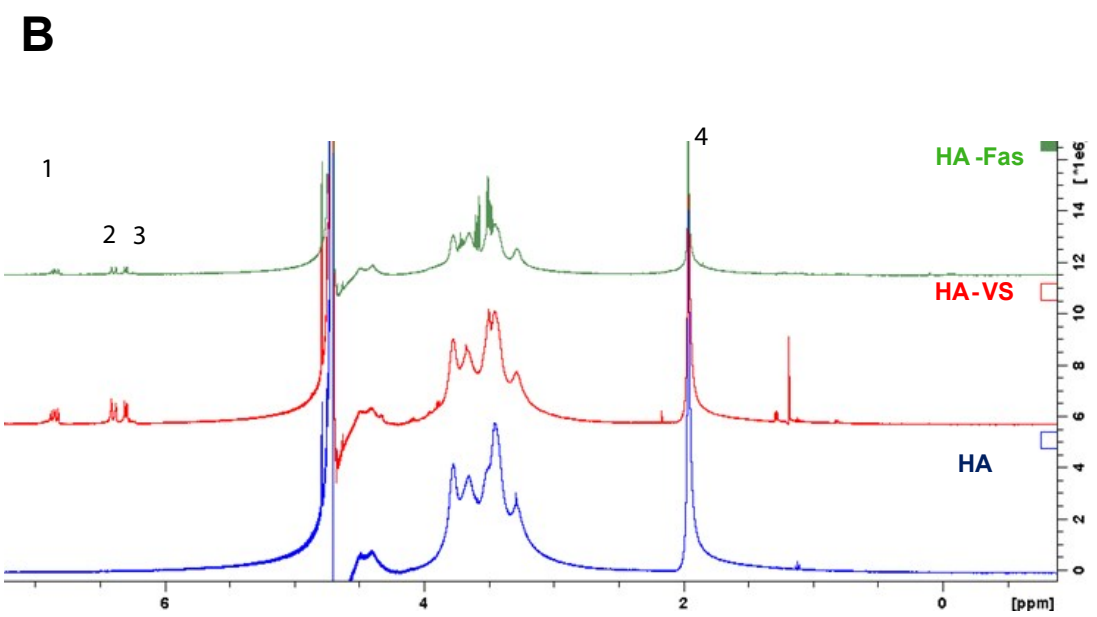

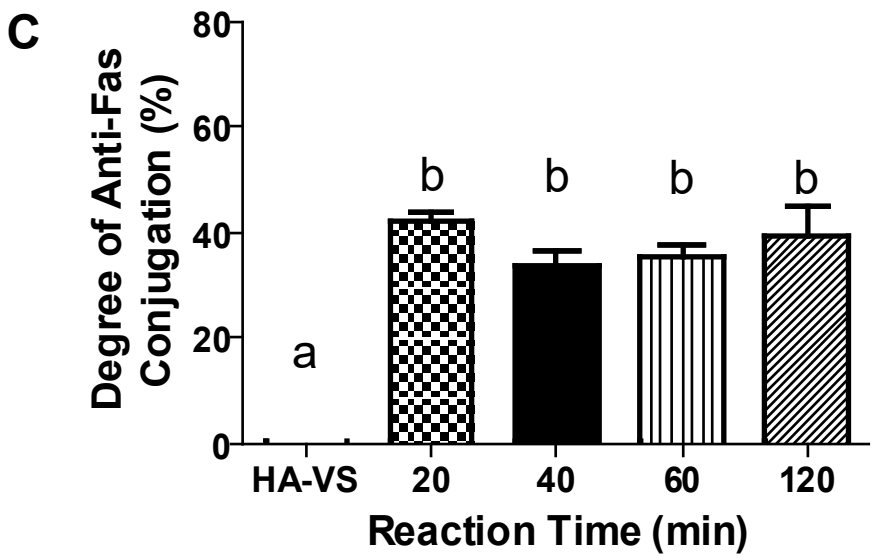

Figure 11

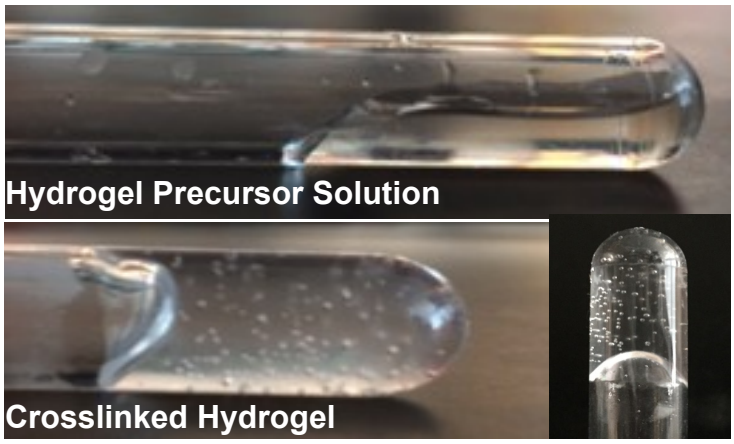

A

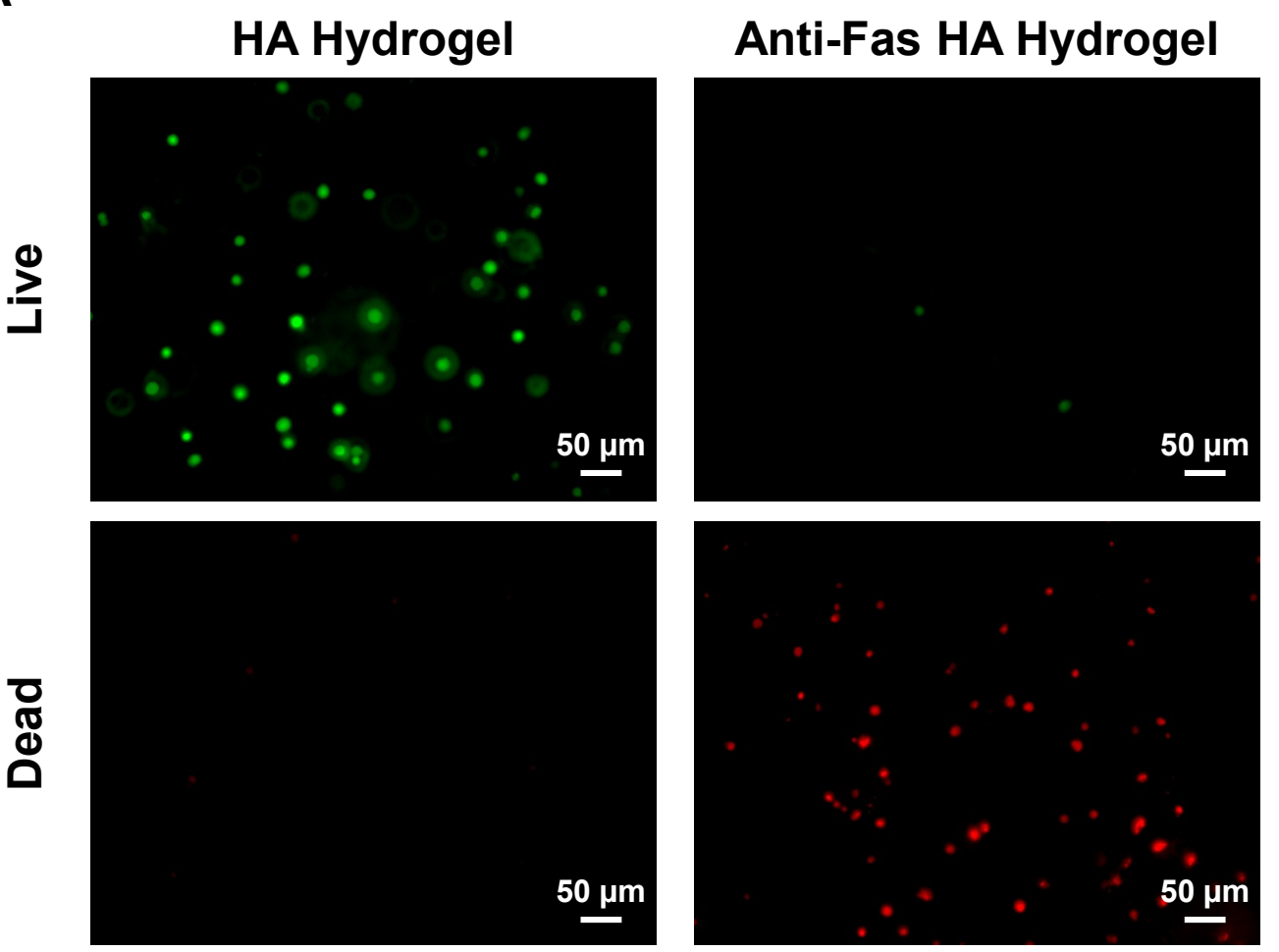

B

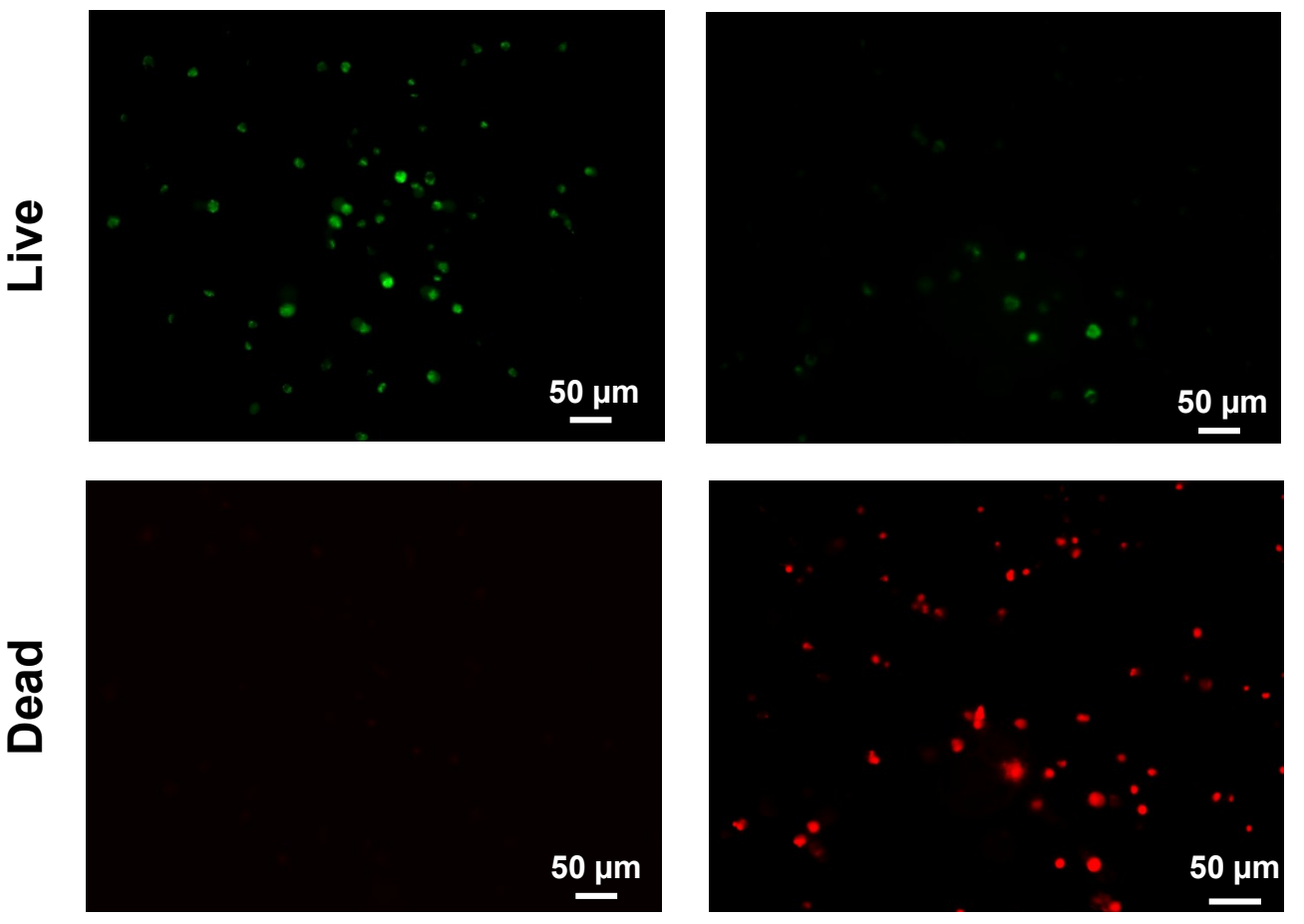

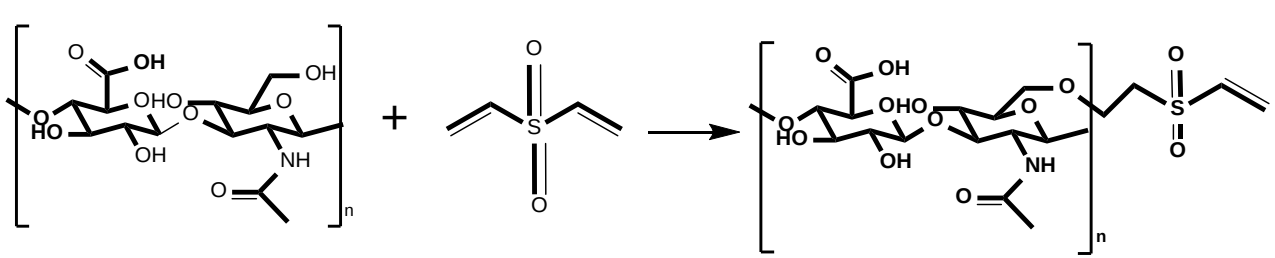

Hyaluronic Acid

Divinyl Sulfone (DVS)

Acrylated HA (HA-Acryl)

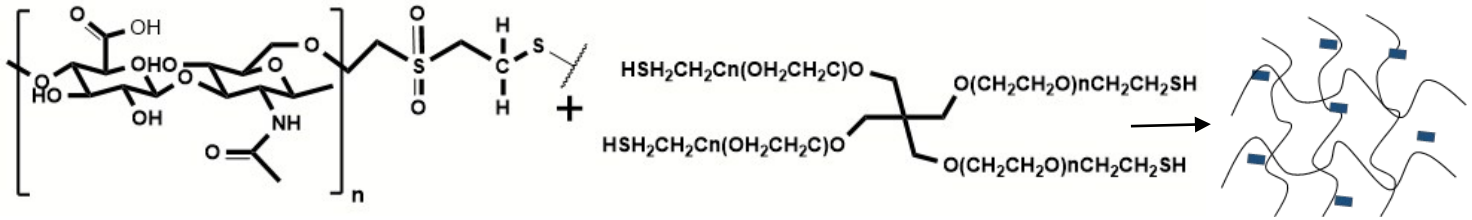

HA-Acryl Conjugated to anti-Fas

4-arm PEG-thiol

HA-Fas